MINISTRY OF SUPPLY

AERONAUTICAL RESEARCH COUNCIL
REPORTS AND MEMORANDA

The Behaviour in Compression of Aluminium Alloy Panels having a Flat Skin with Corrugated Reinforcement

By

E. A. BROOK, M.ENG.

LONDON: HIS MAJESTY'S STATIONERY OFFICE
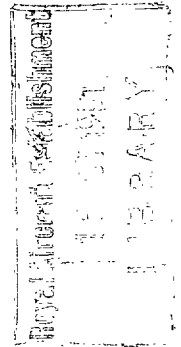
1951

PRICE 8s 6d NET

The Behaviour in Compression of Aluminium Alloy Panels having a Flat Skin with Corrugated Reinforcement

By
E. A. BROOK, M.ENG.

COMMUNICATED BY THE PRINCIPAL DIRECTOR OF SCIENTIFIC RESEACH (AIR),
MINISTRY OF SUPPLY

Summary.—This report describes compression tests on 36 panels, made of D.T.D. 390 and D.T.D. 546. Each panel consisted of a flat skin reinforced with continuous corrugations, and the object of the test was to investigate the effect of rivet pitch and arrangement, corrugation width, and skin and corrugation thickness, on the buckling and failing loads of the panels.

The results indicate that for the thicknesses of skin and corrugations considered in this report, the inter-rivet buckling stress is considerably less than the stress at which the skin between rivets would buckle, when considered as an Euler strut with encastré ends.

1. *Introduction.*—For high-speed aircraft it is desirable to have a form of wing construction which is not only efficient from a strength-weight stand-point, but which will also maintain a smooth surface in the high-speed level-flight condition. One form of construction suitable for this purpose is a flat skin stiffened by continuous corrugations.

This report describes an experimental investigation into the behaviour of this type of construction when loaded in compression. It discusses the effect of rivet pitch, corrugation width, and skin and corrugation thickness for two different types of material, and attempts to indicate the optimum values of these parameters.

It was considered that reliable results could be obtained by testing panels 12 in. long, provided that they embodied at least three sets of corrugations. The centre strip would then indicate the characteristics of any similar single strip forming part of a larger structure.

Thirty-six panels were tested in all.

2. *Description of Specimens.*—Each panel consisted of a flat skin reinforced with three overlapping corrugations. These were chosen so that each side of the corrugated section was of approximately equal length (*see* Figs. 1, 2) and would therefore become unstable at about the same load. The ends of the panels were reinforced across their entire width by strips of material, 2 in. wide, which had the effect of reproducing encastré end conditions.

The ends of the panels were finished parallel and flat to within 0·0005 in.

It was decided not to provide any constraint at the edges of the specimens for the following reasons:—

    (i) It was not considered possible to provide constraint that would reproduce the effect of further corrugations.

    (ii) As the panels failed locally, *i.e.*, either by inter-rivet buckling or buckling between rivet lines, the effect of constraining the edges would in any case be small.

    (iii) Preliminary tests confirmed that edge restraint had little effect on the results.

The specimens were constructed in three groups of twelve panels each. The first group was manufactured out of material to Specification Number D.T.D. 390 with corrugations 3 in. wide, and represented all combinations of the following variables:—

(i) staggered and unstaggered rivets,
(ii) rivet pitches of 0·75 in. and 1·50 in.,
and (iii) combinations of

(a) 12 s.w.G. skin and 14 s.w.G, corrugation,
(b) 14 s.w.G. skin and 16 s.w.G. corrugation,
(c) 16 s.w.G. skin and 18 s.w.G. corrugation.

The second group was manufactured out of material to Specification Number D.T.D. 546 but was identical to the first group in all other respects.

The third group of specimens was constructed out of D.T.D. 390, and was designed on the basis of data obtained from the tests of the first two groups. These tests had shown that, in the majority of cases, those specimens having staggered rivets exhibited a slightly higher standard of strength and resistance to buckling than those with unstaggered rivets ; also that all panels having a rivet pitch of 1·50 in. had failed by inter-rivet buckling, but those with a rivet pitch of 0·75 in. by buckling between rivet lines. This third group of twelve panels was accordingly constructed throughout with staggered rivets. Three panels were made with the same range of sheet thicknesses as the first two groups, a corrugation width of 3·0 in., and a rivet pitch of 1·0 in. The remaining nine covered the same range of sheet thicknesses, but had a corrugation width of 2·25 in., and rivets at 0·75, 1·0 and 1·50 in. pitch.

Details of all the specimens tested are entered in Table 1. General arrangement drawings of typical panels with 3·0 and 2·25 in. wide corrugations, together with detail drawings of the corrugated sections, are shown in Figs. 1, 2 respectively.

3. *Description of Tests.*—Each specimen was tested in compression, by small increments of load up to failure. In all cases the buckling loads, failing loads, and corresponding end deflections of the panels were recorded, and in some cases the stress at which permanent set occurred was also determined.

A preliminary investigation, carried out on Specimen Number E8, using a 70-ton Olsen testing machine, revealed that this machine was not suitable. Subsequent specimens were accordingly tested in a standard 90-ton Richle compound-lever testing machine of the three-screw type. A previous investigation had ensured, that, within specified limits, the movement of the travelling head was parallel to the base plate. The load was applied through two mild-steel plattens having machined surfaces.

Tests were commenced with the upper platten securely attached to the movable head of the machine, and the lower platten resting on a ball mounting which in turn rested on the base plate of the machine. The purpose of the ball mounting was to counteract any slight skew between the ends of the specimens or between the two surfaces of the testing machine. It was assumed that when the applied load attained a value of about two tons, the ball would lock in its socket and the whole system would then behave as if rigid.

To indicate end deflections a dial gauge was fitted at each end of the specimen approximately on its neutral axis. These gauges were attached to steel rods, screwed into the upper platten, with their plungers bearing on the machined surface of the lower platten.

The gauges indicated that the ends of the lower platten tilted when load was applied, and that this tilt continued to increase for loads in excess of two tons. The ball and socket was, therefore, replaced by a rigid mounting which maintained the specimen at the correct height for measuring lateral deflections with apparatus already designed and constructed.

Parallelism of the machined surfaces of the two plattens was obtained by means of shims introduced between the upper platten and the movable head of the machine and was checked after each test by means of a dial gauge mounted on the arm of a scribing block. The plattens were found to remain parallel to within 0·0005 in. throughout the tests. The arrangement is illustrated in Fig. 21.

An endeavour was made to record lateral deflections of the flat skin of the specimens by means of nine dial gauges, with their plungers bearing on the skin at predetermined points. The gauges were mounted on a wooden frame with their centres 3 in. apart in a horizontal direction, and $2\frac{1}{2}$ in. apart in a vertical direction. Four wood screws, let into rebates at the bottom corners of the frame, provided adjustment for levelling. The frame was allowed to rest on the base plate of the machine and was held down by means of lead blocks (*see* Fig. 22). The gauges confirmed the existence of a slight rotational movement of the travelling head of the machine, first detected when investigating its parallel motion. It was not considered that this movement was sufficient to affect adversely the accuracy of the tests.

In consequence of their necessarily wide spacing, the gauges could not be relied upon to detect buckling or to indicate amplitudes and wave lengths, and their use was accordingly abandoned. Instead, the formation of buckles was determined by sliding a steel straight edge along the flat surface of the specimens, allowance being made for any initial deformations. This method was used for Specimens Numbers E1 to E7 and E9 to E12 inclusive.

Two other methods were then used to investigate the incidence of buckling.

The first of these, used for Specimens Numbers E13, E15, E17 and E21 was to employ a sliding curvature gauge, in the form of a dial gauge mounted on a steel slide with movable feet (as on a spherometer). The wave length of the buckle was measured with a steel rule, and the feet of the curvature gauge were set at this distance apart. The gauge was then moved along a wave, and its amplitude was given by half the difference between the maximum and minimum dial readings.

In the second method, used only for Specimen Number 19, the profile of the skin was plotted from the readings of a traverse gauge, consisting of a dial gauge which could slide along a graduated bar attached to the machine (*see* Fig. 26).

The method of sliding a steel straight edge along the plate was reverted to for all other specimens, as this method enabled buckling to be predicted with sufficient accuracy and was, in addition, easier to use.

Analysing the readings obtained with the nine dial gauges on the wooden frame had suggested that the upper platten might be tilting. Accordingly two dial gauges and two angle brackets were arranged to investigate this possibility, thin copper wire connecting the plunger of each gauge to the corresponding lower bracket, as shown in Fig. 23. Owing, however to the difficulty of securing the lower brackets, this set-up was not entirely satisfactory, and Fig. 24 shows the final arrangement adopted. It was assumed that the lower platten could not move relative to the base plate, and the gauges were connected to it directly by copper wire and plasticene. Readings showed that the suspected tilting was not appreciable.

In a number of cases the loads were successively reduced and stepped up to determine the load at which permanent set occurred.

The applied loads were deemed accurate to within 20 lb. All dial gauges were calibrated in $0 \cdot 001$ in., the mean of the readings of two gauges being used to measure end deflections of the panels.

Control tests were carried out on the material used for the manufacture of each component of the various specimens. The results of these tests are entered in Table 2.

4. *Description of Results.*—Details of failing and buckling loads and stresses, and the stresses at which permanent set occurred, together with the type of failure for each specimen, are entered in Table 3. The buckling loads recorded are those at which buckling first became discernible. The stresses entered represent the mean stress developed in the specimen as determined from the formula $f = L/A$,

> where f stress (ton/sq. in.)
>
> L load (tons)
>
> A total cross-sectional area of specimen (sq. in.).

3

In calculating A, the cross-sectional area of the corrugations was taken as developed width times thickness, the actual expressions being,—

(i) for Specimens Numbers E1 to E27

$$A = 9\cdot6t_1 + 12\cdot9t_2$$

(ii) for Specimens Numbers N1 to N9

$$A = 7\cdot35t_1 + 10\cdot3t_2$$

where t_1 thickness of flat skin (in.)

t_2 thickness of corrugation (in.).

The nominal thicknesses of skin and corrugation were used for these calculations as their proximity to the actual thicknesses was in all cases within the limits of accuracy of load and deflection measurements (see Table 2). For three panels on which detailed measurements were made, the actual values of A exceeded the nominal by about 1 per cent.

For ease of comparison, Table 4 shows the failing stresses corrected to the minimum specified 0·1 per cent proof stress of the material, namely, 15 ton/sq. in. for D.T.D.390, and 21 ton/sq. in. for D.T.D.546. This was effected by a simple linear correction as follows:—

$$\text{Corrected stress} = \text{actual stress} \times \frac{\text{minimum specified } 0\cdot1 \text{ per cent proof stress}}{\text{actual } 0\cdot1 \text{ per cent proof stress}}$$

where measured details of wavelengths and amplitudes of buckles at failure, have also been entered in this Table.

All specimens, with the exception of Specimen Number E8, failed by buckling across the entire width of the panel, this exception being attributable to non-parallel movement of the plattens.

In Figs. 3 to 12 the applied loads have been plotted against the corresponding end deflections for all specimens except E8, the deflections at opposite ends of the plattens in this case being too divergent for an accurate average to be taken.

In most cases rivets failed only when inter-rivet buckling occurred and this marked the failing load of the specimen. Failure of the rivets, in general, took place at the countersunk heads on the flat skin.

In the case of Specimen Number E27 inter-rivet buckling was accompanied by failure of the corrugations across the entire width of the panel.

Specimens Numbers N5 and N6 failed by a combination of inter-rivet buckling and buckling between rivet lines and this was accompanied in the case of Specimen Number N6 by failure of the corrugations.

In all other cases no form of buckling occurred other than that initially detected and the corrugations remained undamaged except for buckling of the flanges at the outer edges of the panels.

In some cases the strain was deliberately increased to produce failure of the corrugations but in no case did this result in the specimen carrying an increased load.

Profiles of Specimen Number E19 at different loads are given in Fig. 13.

Photographs of various types of failure are shown in Figs. 23 to 31. In some cases these photographs were taken with the specimen still under strain in the machine. In others, they were taken after the specimens had been removed from the machine, as it was considered that the more effective use of light and shade possible under studio conditions, would outweigh the resulting reduction in the magnitude of the buckles.

4

5. *Discussion of Results.*—5.1. *General.*—The material for Specimens Numbers E1 to E12 was solution treated to bring the 0·1 per cent proof stress down to the region of the minimum specified value of 15 ton/sq. in. This ensured that the proof stresses for skin and corrugation were of the same order for each specimen. The material for Specimens Numbers E13 to E24 was not solution treated, and the 0·1 per cent proof stresses were in most cases about 4 tons/sq. in. above the specified minimum. Control tests were not carried out on the corrugation material for this group, and hence it is not known how closely their proof stresses approached those of the flat skin.

Control tests carried out on the material for Specimens Numbers E25 to E27 and N1 to N9 showed a range in the values of the proof stresses of up to 4 ton/sq. in., *e.g.* the 0·1 per cent proof stress for the skin of Specimen Number E25 was 19·6 ton/sq. in., whilst that for the corrugations was only 16·0 ton/sq. in. When estimating the distribution of stress between skin and corrugation no allowance was made for these differences. This has, in some cases, resulted in the assumption that certain components have been developing unrealistic stresses and has led to very low values of tangent moduli. Where the use of these values has led to obviously incorrect results, these have been pointed out in the text.

All control tests were carried out in tension whereas the panels were tested in compression. Recent investigations have shown that for some materials the proof stresses determined by tension and compression tests are in close agreement, whereas for other materials they differ widely. This phenomenon has not been investigated for material to Specifications Numbers D.T.D.390 and D.T.D.546, and hence it is not possible to take account of it in the analyses of the results.

It has recently been shown that ' clad ' material, as embodied in all the specimens under discussion, exhibits a double modulus of elasticity. This gives rise to two straight lines, of different gradient, in the stress-strain curve, the transition point occurring at the strain at which the cladding begins to yield. For the purpose of this report, the value of Young's Modulus has been taken as the average of these two moduli. Where tangent moduli are quoted at stresses below the proportionality limit of the material, they are one of these two ' subsidiary ' moduli.

In most of the specimens the corrugations were attached to the flat skin by 1/8 in. diameter rivets, but in six cases 5/32 in. rivets were employed. No attempt has been made to differentiate between the results obtained with these two sizes of rivet. No allowance was made, either, for the slight change in the general form of the corrugations of the N specimens from those of the E series (*see* Figs. 1, 2).

All loads have been corrected in accordance with the National Physical Laboratory calibration curves for the testing machine. Figs. 3 to 12 do not embody this correction.

The degree of initial flatness of the sheets varied considerably. This not only tended to accelerate the incidence of buckling in some cases, but also hampered its detection. Fig. 13 shows the initial profile of Specimen Number E19 which was one of the flattest panels tested.

The effect of the ratio of skin to corrugation thickness is not considered in this report, as all the conclusions relate to a ratio of about 1·3. The actual ratios were 1·25, 1·30 and 1·33.

5.2. *Average Failing and Buckling Stresses.*—In general, staggering the rivets resulted in a slight increase in the failing and buckling stresses.

The average failing stresses of the specimens increased with the thickness of the flat plate for Specimens Numbers E1 to E24 and N7 to N9 as shown in Table 4. The exceptions are probably attributable to the different properties of the skin and corrugations materials. The failing stresses, corrected to the minimum specified 0·1 per cent proof stress, as previously described, have been plotted against skin thickness in Fig. 14. It will be seen that in general, the increase is linear.

Higher stresses were obtained with close pitch rivets.

Material to Specification Number D.T.D.390 in all cases developed a higher ratio of average failing stress/minimum specified $0 \cdot 1$ per cent proof stress than that to D.T.D.546.

The average buckling stresses also varied linearly with skin thickness, but for the exceptions noted above. After the incidence of inter-rivet buckling a small increment of load usually produced failure, whereas after buckling between rivet lines the specimens withstood a considerable increase of load.

Buckling stresses are shown in Table 3, and it is noticeable that the ratio buckling stress/failing stress is lower for D.T.D.546 than for D.T.D.390. The buckling stresses have not been corrected to a constant proof stress as they are, in the main, well below the $0 \cdot 1$ per cent proof stress.

5.3. *Inter Rivet Buckling.*—All specimens with a rivet pitch of $1 \cdot 50$ in., some with a rivet pitch of $1 \cdot 0$ in., but none with a rivet pitch of $0 \cdot 75$ in., failed by inter-rivet buckling.

For inter-rivet buckling it has been assumed that the portion of skin between two rivets behaves as a strut and follows the Euler formula,

$$i.e., \ L = C \pi^2 EI/l^2,$$

where L the load on the strut (lb),

      C a constant depending upon the degree of end fixity,

      E Young's Modulus (lb/sq. in.),

      I minimum second moment of area of skin (in.^{4}),

      l length of strut, rivet pitch (in.).

Therefore, $f_b = \dfrac{L}{A_s} = C \pi^2 E K^2/l^2$

where f_b buckling stress (lb/sq. in.),

      A_s cross-sectional area of skin (sq. in.),

      K minimum radius of gyration of section (in.).

But $K^2 = t_1^2/12$, where t_1 is the thickness of skin (in.),

therefore, $C = 12 f_b \, l^2/\pi^2 E \, t_1^2$.

The right hand side of this equation can be evaluated from test data, and values of C, obtained in this manner, are entered in Table 5.

If the buckling stress exceeds the proportionality limit of the skin material, the tangent modulus at the buckling stress should be used in place of Young's modulus, and C' in place of C, where

$$C' = \frac{12 f_b \, l^2}{\pi^2 E' \, t_1^2},$$

and E' tangent modulus at the buckling stress (lb/sq. in.).

Values of C' are also entered in Table 5.

Previous practice has in general been based on the assumption that rivets produced encastré end conditions in the flat plate, and C was thus taken as $4 \cdot 0$. Table 5 clearly indicates that the values of C and C', determined by this series of tests, are of the order of $1 \cdot 5$, and the rivets therefore produce end conditions somewhere between encastré and simple support.

The value for C' of $31 \cdot 4$ for Specimen Number N2 is obviously incorrect, and is excluded from subsequent analyses. This absurdly high value is due to an extremely low value of the tangent modulus, and is probably due to the fact that for this specimen the stress-strain curves for skin and corrugation material were markedly different.

6

The values of C increase slightly with reduction in rivet pitch and/or corrugation width. This effect can be explained by assuming each rivet to exert a restraining influence on the flat skin over a field of constant radius. The effect of reducing the distance between rivets is then to reduce the ratio length of unrestrained skin/distance between supports and hence increase C. C also decreases slightly with increase in skin thickness.

The behaviour of C' is not quite as consistent as that of C, because the stress-strain curves for skin and corrugation were not identical in each case, and hence the values of the buckling stresses in the skin, used to obtain tangent moduli, were not strictly correct. The use of tangent moduli does, however, take account of the differing properties of the two materials, which, although they have similar Young's Moduli, have different proof stresses.

The values of C and C' are remarkably consistent and the following generalizations can be made for a ratio of skin thickness/corrugation thickness of about $1 \cdot 3$, and skin thickness between $0 \cdot 064$ in. and $0 \cdot 104$ in.

Width of corrugation (in.)	Rivet pitch (in.)	C	C'
3·0	1·5	1·14	1·19
2·25	1·5	1·55	1·74

Insufficient tests were carried out to determine values for a rivet pitch of $1 \cdot 0$ in.

To estimate the stress, f_c, in the corrugations at failure, it was assumed that after the flat skin had buckled, the load which it took remained constant.

Therefore

$$L = A_s f_b + A_c f_c$$

$$\text{or } f_c = \frac{L - A_s f_b}{A_c}$$

where L failing load (tons),

A_s cross-sectional area of skin (sq. in.),

A_c cross-sectional area of corrugations (sq. in.),

f_b average stress in panel, at buckling (tons/sq. in.).

Values of f_c, so obtained, are entered in Table 7, together with the ratio f_c/f_b.

When the incidence of buckling and failure occurred at the same load (as for Specimens Numbers N2 and N3) it was assumed that the skin and corrugations were each subject to the same stress.

The failing stresses in the corrugations are plotted against skin thickness in Fig. 17. The results for Specimen Number E25 have been neglected as obviously false.

5.4. *Buckling Between Rivet Lines (quilting)*.—All specimens having a rivet pitch of $0 \cdot 75$ in. failed by buckling between rivet lines, and some specimens with a rivet pitch of $1 \cdot 0$ in. also failed in this manner. Specimens Numbers N5 and N6 appeared to fail by a combination of inter rivet and quilted buckling, but subsequent analysis showed that they fell into the category of quilted buckling.

For buckling between rivet lines the following formula has been used

$$f_b = KE\left(\frac{t}{b}\right)^2,$$

$$\text{or } K = \frac{f_b}{E}\left(\frac{b}{t_1}\right)^2,$$

where f_b average buckling stress (lb/sq. in.),

$\quad\quad K$ a constant,

$\quad\quad E$ Young's Modulus (lb/sq. in.),

$\quad\quad b$ distance between rivet lines (in.),

$\quad\quad t_1$ thickness of flat skin (in.),

or using tangent moduli $K' = \dfrac{f_b}{E'}\left(\dfrac{b}{t_1}\right)^2,$

where $E' =$ tangent modulus at buckling stress (lb/sq.in.²).

Mathematical analysis indicates that the buckling stress is probably a function of $(EE')^{1/2}$. That this is not unreasonable can be seen from the fact that if the longitudinal stress is above the proportionality limit the tangent modulus should be used, whereas the complementary transverse stress will probably be below the proportionality limit, and hence Young's Modulus is appropriate.

Values of K, K' and $(KK')^{1/2}$ have been entered in Table 6 and K has been plotted against skin thickness in Fig. 18. K decreases uniformly with increase of skin thickness and is lower for D.T.D.546 than D.T.D.390. The staggering of rivets has no appreciable effect on K.

Whereas it is more mathematically correct to use (KK') than K for design purposes, values of the former show much more scatter. This is probably due to the difference in properties of skin and corrugation materials, and since this difference will be present, to some extent, in all constructions, it is suggested that for design purposes it is sufficiently accurate to use K.

Table 8 shows the estimated values of the failing stresses in both skin and corrugation for quilted buckling.

At failure $L = f_c A_c + f_s A_s$,

where L failing load (tons),

$\quad\quad f_c$ failing stress in corrugations (ton/sq. in.),

$\quad\quad f_s$ failing stress in skin (ton/sq. in.),

$\quad\quad A_c$ cross-sectional area of corrugations (sq. in.),

$\quad\quad A_s$ cross-sectional area of skin (sq. in.).

In the above equation, L, A_c and A_s are known. Also from Royal Aeronautical Society *Stressed Skin Data Sheet* Number 02.01.03, the ratio $f_c/f_s = f$ (edge)$/f$ (average) can be obtained for any ratio of corrugation width/skin thickness $(= b/t_1)$. By choosing an arbitrary value of f_c and reading, from the data sheet, the corresponding value of f_s, it is possible to evaluate the right hand side of the above equation. Balance of the equation is then obtained by successive approximations of f_c, and the final values of f_c and f_s are entered in Table 8.

These values of f_c and f_s are plotted against skin thickness in Figs. 19 and 20 respectively. With the exception of N4, the failing stresses in the skin increase uniformly with skin thickness for different combinations of corrugation width and material. The slight variations of failing stresses in the corrugation probably reflect changes in the ratio skin thickness/corrugation thickness.

6. *Conclusions.*—The conclusions are based on a ratio of skin thickness/corrugation thickness of the order of $1 \cdot 3$ and a range of skin thickness from $0 \cdot 064$ in. to $0 \cdot 104$ in. They are as follows :—

(i) Slightly better characteristics are obtained with staggered rivets than with unstaggered rivets.

(ii) For inter-rivet buckling it may be assumed that the skin maintains its buckling strength up to failure ; this type of buckling occurs at a higher percentage of the failing load than quilted buckling.

(iii) D.T.D.546 sustains a higher failing stress than D.T.D.390, but the ratio failing stress/ $0 \cdot 1$ per cent. Proof Stress is lower for D.T.D. 546 than for D.T.D.390.

(iv) For inter-rivet buckling the Euler Constant, C, is of the order of $1 \cdot 5$ and not $4 \cdot 0$ as often assumed. The value of C increases slightly with reduction in corrugation width, rivet pitch, and/or skin thickness. The values are substantially the same for D.T.D.390 and D.T.D.546.

(v) If initial deformations and differences in properties of skin and corrugation materials are not taken into account, reasonably consistent results are obtained by assuming that $f_b = KE(t_1/b)^2$; K decreases uniformly with increase of skin thickness. For the panels tested the extreme values are $5 \cdot 6$ and $2 \cdot 3$.

REFERENCES

No.	Author.	Title, etc.
1	S. Timoshenko	Theory of Elastic Stability. McGraw-Hill Publishing Co. 1936.
2	J. B. B. Owen and G. M. Jones	The Compressive Strength of Metal Covering Reinforced by Corrugated Sheeting. R.A.E. Report AD 3128. A.R.C. No. 4562. October, 1939.

TABLE 1

Details of Specimens

Specimen Number	Material Specification Number	Width of Corrugations (in.) b	Arrangement of Rivets	Diameter of Rivets (in.)	Rivet Pitch (in.)	Flat Plate t_1 S.W.G.	Corrugation t_2 S.W.G.	Calculated cross-Sectional Area sq. in. A
E1 ..	D.T.D.390	3·0	Unstaggered	1/8	0·75	12	14	2·03
E2 ..	D.T.D.390	3·0	Unstaggered	1/8	1·50	12	14	2·03
E3 ..	D.T.D.390	3·0	Unstaggered	1/8	0·75	14	16	1·594
E4 ..	D.T.D.390	3·0	Unstaggered	1/8	1·50	14	16	1·594
E5 ..	D.T.D.390	3·0	Unstaggered	1/8	0·75	16	18	1·233
E6 ..	D.T.D.390	3·0	Unstaggered	1/8	1·50	16	18	1·233
E7 ..	D.T.D.390	3·0	Staggered	1/8	0·75	12	14	2·03
E8 ..	D.T.D.390	3·0	Staggered	1/8	1·50	12	14	2·03
E9 ..	D.T.D.390	3·0	Staggered	1/8	0·75	14	16	1·594
E10 ..	D.T.D.390	3·0	Staggered	1/8	1·50	14	16	1·594
E11 ..	D.T.D.390	3·0	Staggered	1/8	0·75	16	18	1·233
E12 ..	D.T.D.390	3·0	Staggered	1/8	1·50	16	18	1·233
E13 ..	D.T.D.546	3·0	Unstaggered	1/8	0·75	12	14	2·03
E14 ..	D.T.D.546	3·0	Unstaggered	1/8	1·50	12	14	2·03
E15 ..	D.T.D.546	3·0	Unstaggered	1/8	0·75	14	16	1·594
E16 ..	D.T.D.546	3·0	Unstaggered	1/8	1·50	14	16	1·594
E17 ..	D.T.D.546	3·0	Unstaggered	1/8	0·75	16	18	1·233
E18 ..	D.T.D.546	3·0	Unstaggered	1/8	1·50	16	18	1·233
E19 ..	D.T.D.546	3·0	Staggered	1/8	0·75	12	14	2·03
E20 ..	D.T.D.546	3·0	Staggered	1/8	1·50	12	14	2·03
E21 ..	D.T.D.546	3·0	Staggered	1/8	0·75	14	16	1·594
E22 ..	D.T.D.546	3·0	Staggered	1/8	1·50	14	16	1·594
E23 ..	D.T.D.546	3·0	Staggered	1/8	0·75	16	18	1·233
E24 ..	D.T.D.546	3·0	Staggered	1/8	1·50	16	18	1·233
E25 ..	D.T.D.390	3·0	Staggered	1/8	1·0	12	14	2·03
E26 ..	D.T.D.390	3·0	Staggered	1/8	1·0	14	16	1·594
E27 ..	D.T.D.390	3·0	Staggered	1/8	1·0	16	18	1·233
N1 ..	D.T.D.390	2·25	Staggered	5/32	1·0	12	14	1·588
N2 ..	D.T.D.390	2·25	Staggered	5/32	1·0	14	16	1·247
N3 ..	D.T.D.390	2·25	Staggered	1/8	1·0	16	18	0·965
N4 ..	D.T.D.390	2·25	Staggered	5/32	0·75	12	14	1·588
N5 ..	D.T.D.390	2·25	Staggered	5/32	0·75	14	16	1·247
N6 ..	D.T.D.390	2·25	Staggered	1/8	0·75	16	18	0·965
N7 ..	D.T.D.390	2·25	Staggered	5/32	1·50	12	14	1·588
N8 ..	D.T.D.390	2·25	Staggered	5/32	1·50	14	16	1·247
N9 ..	D.T.D.390	2·25	Staggered	1/8	1·50	16	18	0·965

TABLE 2

Results of Control Tests

Specimen number	Location	Thickness (in.)	Proportion-ality Limit (ton/sq. in.)	0·1 per cent. Proof Stress (ton/sq. in.)	0·2 per cent. Proof Stress (ton/sq. in.)	0·5 per cent. Proof Stress (ton/sq. in.)	Maximum Stress (ton/sq.in.)	E (lb/sq. in. $\times 10^6$)
E1 ..	Skin	0·1061	10·8	16·5	16·7	17·5	27·1	9·0
E1 ..	Corrugation	0·0796	11·5	15·4	16·0	17·3	26·8	9·5
E2 ..	Skin	0·1046	11·5	16·0	16·5	17·7	27·3	9·3
E2 ..	Corrugation	0·0797	11·3	15·3	15·4	16·6	26·2	10·1
E3 ..	Skin	0·0796	10·1	15·4	16·2	17·3	26·1	9·4
E3 ..	Corrugation	0·0631	11·1	16·0	16·5	17·8	27·9	9·4
E4 ..	Skin	0·079	12·6	14·8	15·7	16·7	26·0	9·1
E4 ..	Corrugation	0·063	13·4	15·35	16·0	17·2	26·7	9·1
E5 ..	Skin	0·0625	11·3	15·9	16·5	17·7	27·7	9·7
E5 ..	Corrugation	0·0510	8·1	14·8	15·8	17·2	26·6	9·6
E6 ..	Skin	0·0625	11·1	15·8	16·5	17·8	27·3	9·7
E6 ..	Corrugation	0·0510	8·0	15·3	16·0	17·1	26·7	10·2
E7 ..	Skin	0·106	14·3	15·72	16·1	17·3	26·1	9·7
E7 ..	Corrugation	0·079	13·4	15·45	16·1	17·0	26·0	9·3
E8 ..	Skin	0·1049	12·7	16·1	16·8	17·8	27·3	9·0
E8 ..	Corrugation	0·0798	10·5	15·1	15·8	17·0	28·5	9·7
E9 ..	Skin	0·0796	10·1	15·4	16·1	17·2	26·2	9·8
E9 ..	Corrugation	0·0637	10·3	15·7	16·5	17·6	27·5	9·4
E10 ..	Skin	0·078	16·4	19·5	20·1	21·0	27·5	10·4
E10 ..	Corrugation	0·062	14·1	15·85	16·3	17·3	27·2	9·7
E11 ..	Skin	0·065	16·7	18·8	19·3	20·1	27·2	9·4
E11 ..	Corrugation	0·051	12·0	14·5	15·4	16·7	25·2	9·0
E12 ..	Skin	0·062	13·0	15·75	16·5	17·5	27·3	9·5
E12 ..	Corrugation	0·051	13·2	15·6	16·2	17·0	25·5	8·8
E13 ..	Skin	0·102	12·3	25·0	26·2	27·3	29·7	9·7
E13 ..	Corrugation	—	—	—	—	—	—	—
E14 ..	Skin	0·102	12·0	24·6	25·5	27·0	29·6	9·95
E14 ..	Corrugation	—	—	—	—	—	—	—
E15 ..	Skin	0·079	13·7	24·7	25·6	26·8	30·2	10·2
E15 ..	Corrugation	—	—	—	—	—	—	—
E16 ..	Skin	0·079	13·6	25·0	26·0	27·1	30·2	9·8
E16 ..	Corrugation	—	—	—	—	—	—	—
E17 ..	Skin	0·062	13·2	25·0	26·0	27·1	30·2	9·5
E17 ..	Corrugation	—	—	—	—	—	—	—
E18 ..	Skin	0·064	18·4	25·0	26·0	26·9	30·0	9·7
E18 ..	Corrugation	—	—	—	—	—	—	—
E19 ..	Skin	0·102	11·6	24·4	25·8	27·0	29·9	10·1
E19 ..	Corrugation	—	—	—	—	—	—	—
E20 ..	Skin	0·102	10·6	24·7	26·0	26·9	29·8	9·5
E20 ..	Corrugation	—	—	—	—	—	—	—
E21 ..	Skin	0·078	10·3	24·4	25·5	26·4	30·0	10·0
E21 ..	Corrugation	—	—	—	—	—	—	—
E22 ..	Skin	0·080	15·7	24·7	25·6	26·7	29·8	9·7
E22 ..	Corrugation	—	—	—	—	—	—	—
E23 ..	Skin	0·065	18·8	25·2	26·2	26·8	30·0	9·7
E23 ..	Corrugation	—	—	—	—	—	—	—
E24 ..	Skin	0·065	12·4	24·3	25·3	26·4	30·1	10·7
E24 ..	Corrugation	—	—	—	—	—	—	—
E25 ..	Skin	0·104	15·8	19·6	20·2	21·0	27·20	9·9
E25 ..	Corrugation	0·079	13·4	16·0	16·7	17·8	26·30	10·8
E26 ..	Skin	0·082	13·0	15·5	16·7	17·75	26·10	10·1
E26 ..	Corrugation	0·065	13·0	15·0	19·3	20·7	29·85	10·6
E27 ..	Skin	0·066	14·5	17·75	19·1	20·2	26·80	10·1
E27 ..	Corrugation	0·051	17·5	19·5	20·8	21·5	27·00	10·0

TABLE 2—*contd.*

Results of Control Tests

Specimen number		Location	Thickness (in.)	Proportion-ality Limit (ton/sq. in.)	0·1 per cent. Proof Stress (ton/sq. in.)	0·2 per cent. Proof Stress (ton/sq. in.)	0·5 per cent. Proof Stress (ton/sq. in.)	Maximum Stress (ton/sq. in.)	E (lb/sq. in. $\times 10^6$)
N1	..	Skin	0·105	14·3	16·7	17·2	18·2	27·30	9·9
N1	..	Corrugation	0·087	15·1	17·0	17·6	18·8	26·00	10·1
N2	..	Skin	0·080	14·5	16·8	17·1	18·0	26·90	10·1
N2	..	Corrugation	0·065	14·6	17·5	18·5	19·9	29·65	11·2
N3	..	Skin	0·063	14·5	15·5	18·0	18·8	26·65	9·9
N3	..	Corrugation	0·049	15·7	17·3	18·5	20·2	28·45	10·2
N4	..	Skin	0·105	14·0	15·5	16·7	18·2	26·90	8·0
N4	..	Corrugation	0·088	12·6	15·0	16·0	17·3	27·40	10·4
N5	..	Skin	0·080	9·8	15·5	17·0	17·5	27·05	10·4
N5	..	Corrugation	0·066	14·0	16·3	17·7	19·5	29·90	10·6
N6	..	Skin	0·062	13·1	15·7	16·6	17·6	26·65	10·2
N6	..	Corrugation	0·048	13·2	17·3	18·3	19·5	28·40	9·5
N7	..	Skin	0·104	10·7	15·5	17·5	18·1	26·81	10·2
N7	..	Corrugation	0·084	11·0	14·7	15·2	16·4	26·60	9·2
N8	..	Skin	0·081	14·8	18·0	18·8	19·4	26·18	9·4
N8	..	Corrugation	0·066	12·6	17·5	18·5	19·7	29·35	10·4
N9	..	Skin	0·064	13·8	16·0	17·2	18·5	27·40	10·1
N9	..	Corrugation	0·049	12·9	15·5	17·3	18·3	27·85	10·1

TABLE 3

Results of Tests

Specimen Number	Buckling Load (tons)	Buckling Stress (ton/ sq. in.) f_b	Permanent Set Stress (ton/ sq. in.)	Failing Load (tons) L	Failing Stress (ton/ sq. in.) f	Type of Buckling	Load Deflection Graph	Remarks
E1 ..	26·3	12·95	—	34·0	16·7	Quilted	3	Buckled slightly as Euler strut at 26 tons.
E2 ..	29·9	14·75	—	30·9	15·2	Inter-rivet	3	Flat skin started to leave corrugation, at one edge, at 24 tons.
E3 ..	19·4	12·15	—	23·8	14·9	Quilted	4	Slight bowing as Euler strut at 19 tons.
E4 ..	18·4	11·5	—	18·5	11·6	Inter-rivet	4	One rivet failed at 18 tons. Three more one minute later at same load.
E5 ..	12·3	9·93	—	16·05	13·0	Quilted	5	
E6 ..	10·2	8·3	—	13·25	10·7	Inter-rivet	5	One rivet failed at 13 tons.
E7 ..	31·5	15·45	—	33·2	16·3	Quilted	3	Commenced buckling concave outwards at sides and convex outwards at centre at 31 tons.
E8 ..	—	—	—	22·85	11·25	Inter-rivet	—	Unrepresentative failure—plattens did not remain parallel.
E9 ..	19·6	12·28	—	22·25	14·0	Quilted	4	
E10 ..	21·3	13·4	—	22·0	13·8	Inter-rivet	4	Four rivets failed at 21·75 tons. One further rivet failed later at same load.
E11 ..	13·3	10·81	—	17·3	14·0	Quilted	5	
E12 ..	8·25	6·7	—	12·5	10·1	Inter-rivet	5	
E13 ..	24·4	11·98	14·6	40·7	20·1	Quilted	6	Load inadvertently increased from 31 to 40 tons in one step.
E14 ..	36·5	17·9	17·9	38·2	18·8	Inter-rivet	6	Buckled between two rows of rivets. Seven rivets failed.
E15 ..	16·3	10·2	12·1	28·9	18·1	Quilted	7	Measurement of buckles hindered by initial deformations of flat skin.
E16 ..	20·4	12·8	12·8	20·8	13·0	Inter-rivet	7	Four rivets failed at 20·5 tons.
E17 ..	8·3	6·7	7·25	18·5	15·0	Quilted	8	
E18 ..	10·2	8·3	8·3	15·0	12·2	Inter-rivet	8	Five rivets failed at 14·75 tons.
E19 ..	30·5	15·0	15·1	42·2	20·7	Quilted	6	This was one of the best specimens tested as regards initial flatness of the skin.
E20 ..	32·2	15·9	15·9	36·75	18·1	Inter-rivet	6	Five rivets failed at 36·25 tons.
E21 ..	17·4	10·88	13·45	28·4	17·8	Quilted	7	Measurement of buckles hindered by initial deformations of flat skin.
E22 ..	19·4	12·1	12·1	23·6	14·8	Inter-rivet	7	Failed by zig-zag inter-rivet buckling. Four rivets failed.
E23 ..	11·2	9·08	—	19·05	15·3	Quilted	8	
E24 ..	10·2	8·3	8·3	14·5	11·8	Inter-rivet	8	One rivet failed at 14·25 tons.
E25 ..	14·55	7·2	15·17	34·03	16·76	Inter-rivet	9	Four rivets failed by shearing of heads.
E26 ..	13·7	8·6	14·80	24·84	15·58	Quilted	9	
E27 ..	15·4	12·5	12·55	16·92	13·72	Inter-rivet	9	Buckling accompanied by failure of corrugations across width of panel.
N1 ..	21·6	13·63	18·00	30·24	18·92	Quilted	10	
N2 ..	24·90	19·94	19·94	24·90	19·94	Inter-rivet	11	No evidence of buckling prior to failure. Two rivets failed.
N3 ..	14·9	15·46	15·46	14·90	15·46	Inter-rivet	12	No evidence of buckling prior to failure.
N4 ..	28·1	17·69	18·26	29·88	18·81	Quilted	10	Measurement of buckles hindered by initial deformations of flat skin.
N5 ..	24·2	19·44	19·44	24·64	19·76	Quilted & Inter rivet	11	Two rivets failed on line of inter-rivet buckling.
N6 ..	13·7	14·2	16·04	15·94	16·53	Quilted & Inter-rivet	12	Buckling accompanied by failure of corrugations across width of panel.
N7 ..	23·6	14·85	.17·68	28·09	17·68	Inter-rivet	10	Two rivets failed.
N8 ..	19·0	15·3	16·32	20·35	16·65	Inter-rivet	11	Two rivets failed.
N9 ..	10·05	10·42	10·42	12·20	12·65	Inter-rivet	12	

TABLE 4

Corrected Failing Stresses and Dimensions of Buckles

Specimen Number	Corrected Failing Stress (ton/sq. in.)	Wave Length of Buckle at Failure (in.)	Amplitude of Buckle at Failure (in. $\times 10^{-3}$)	Photograph of Failure.
E1	15·2	—	—	—
E2	14·2	—	—	Fig. 27
E3	14·5	—	—	—
E4	11·8	—	—	—
E5	12·3	—	—	—
E6	10·2	—	—	—
E7	15·5	—	—	Fig. 29
E8	10·5	—	—	—
E9	13·6	—	—	—
E10	10·6	—	—	Fig. 28
E11	11·2	—	—	—
E12	9·8	—	—	—
E13	16·9	4·75	82·0	—
E14	16·1	—	—	—
E15	15·4	4·25	150·0·	—
E16	10·9	—	—	—
E17	12·6	4·5	78·0	—
E18	10·2	—	—	Fig. 23
E19	17·8	—	—	Fig. 26
E20	15·4	—	—	—
E21	15·3	4·5	89·5	Fig. 25
E22	12·6	—	—	—
E23	12·8	—	—	—
E24	10·2	—	—	Fig. 24
E25	12·8	—	—	—
E26	15·1	—	—	—
E27	11·6	—	—	Fig. 31
N1	17·0	—	—	—
N2	17·8	—	—	—
N3	15·0	—	—	—
N4	18·2	—	—	Fig. 30
N5	19·1	—	—	—
N6	15·8	—	—	—
N7	17·1	—	—	—
N8	13·9	—	—	—
N9	10·5	—	—	—

TABLE 5

Values of Inter-Rivet Buckling Constants

Specimen Number	Rivet Pitch (in.) l	Width of Corrugation (in.) b	Nominal Skin Thickness (in.) t_1	Buckling Stress (lb.sq/in.) f_b	E (lb./sq. in. $\times 10^6$)	E' (lb./sq. in. $\times 10^6$)	C	C'
E2	1·5	3·0	0·104	33,000	9·3	5·44	0·90	1·53
E4	1·5	3·0	0·080	25,800	9·1	=E	1·22	1·22
E6	1·5	3·0	0·064	18,550	9·7	=E	1·28	1·28
E10	1·5	3·0	0·080	30,000	10·4	=E	1·23	1·23
E12	1·5	3·0	0·064	14,950	9·5	=E	1·05	1·05
E14	1·5	3·0	0·104	40,100	9·95	8·6	1·02	1·18
E16	1·5	3·0	0·080	28,600	9·8	=E	1·25	1·25
E18	1·5	3·0	0·064	18,600	9·7	=E	1·28	1·28
E20	1·5	3·0	0·104	35,600	9·5	9·0	0·96	1·01
E22	1·5	3·0	0·080	27,200	9·7	=E	1·20	1·20
E24	1·5	3·0	0·064	18,600	10·7	=E	1·16	1·16
E25	1·0	3·0	0·104	16,080	9·9	=E	1·83	1·83
E27	1·0	3·0	0·064	28,000	10·1	7·3	0·83	1·15
N2	1·0	2·25	0·080	44,600	10·1	0·27	0·84	31·4
N3	1·0	2·25	0·064	34,600	9·9	6·52	1·04	1·57
N7	1·5	2·25	0·104	33,250	10·2	7·9	0·83	1·07
N8	1·5	2·25	0·080	34,250	9·4	8·4	1·56	1·75
N9	1·5	2·25	0·064	23,300	10·1	9·0	1·54	1·73

TABLE 6

Values of Quilted Buckling Constants

Specimen Number	Width of Corrugations (in.) b	Nominal Skin Thickness (in.) t_1	Buckling Stress (lb./sq. in.) f_b	E (lb./sq. in. $\times 10^6$)	E' (lb./sq. in. $\times 10^6$)	K	K'	$(KK')^{1/2}$
E1	3·0	0·104	29,000	9·0	8·05	2·68	3·0	2·84
E3	3·0	0·080	27,200	9·4	7·2	4·08	5·32	4·65
E5	3·0	0·064	22,200	9·7	=E	5·04	5·04	5·04
E7	3·0	0·104	34,600	9·7	1·39	2·97	20·8	7·85
E9	3·0	0·080	27,500	9·8	7·2	3·94	5·37	4·60
E11	3·0	0·064	24,200	9·4	=E	5·66	5·66	5·66
E13	3·0	0·104	26,800	9·7	=E	2·31	2·31	2·31
E15	3·0	0·080	22,800	10·2	=E	3·15	3·15	3·15
E17	3·0	0·064	15,000	9·5	=E	3·47	3·47	3·47
E19	3·0	0·104	33,600	10·1	7·25	2·78	3·86	3·28
E21	3·0	0·080	24,400	10·0	8·75	3·43	3·93	3·66
E23	3·0	0·064	20,300	9·7	=E	4·60	4·60	4·60
E26	3·0	0·080	19,230	10·1	=E	2·69	2·69	2·69
N1	2·25	0·080	30,500	9·9	7·18	2·44	3·37	2·86
N4	2·25	0·104	39,700	8·0	0·64	2·31	28·9	8·18
N5	2·25	0·080	43,600	10·4	2·85	3·31	12·1	6·32
N6	2·25	0·064	31,800	10·2	7·55	3·85	5·21	4·43

TABLE 7

Calculated Stresses in Corrugations at Inter-Rivet Failure

Specimen Number	Failing Load (tons) L	Buckling Stress (ton/sq. in.) f_b	Cross-Sectional Area of flat skin (sq. in.) A_s	Cross-Sectional Area of Corrugations (sq. in.) A_c	Calculated Stress in Corrugations at Failure (ton/sq. in.) f_c	$\dfrac{f_c}{f_b}$
E2	30·9	14·75	1·0	1·03	15·7	1·06
E4	18·5	11·5	0·768	0·826	11·7	1·02
E6	13·25	8·3	0·614	0·619	13·2	1·59
E10	22·0	13·4	0·768	0·826	14·15	1·06
E12	12·5	6·7	0·614	0·619	13·55	2·02
E14	38·2	17·9	1·0	1·03	19·7	1·10
E16	20·8	12·8	0·768	0·826	13·3	1·04
E18	15·0	8·3	0·614	0·619	16·0	1·93
E20	36·75	15·9	1·0	1·03	20·25	1·27
E22	23·6	12·1	0·768	0·826	17·3	1·43
E24	14·5	8·3	0·614	0·619	15·2	1·83
E25	34·03	7·2	1·0	1·03	26·1	3·63
E27	16·92	12·5	0·614	0·619	14·9	1·19
N2	24·90	19·94	0·587	0·661	19·94	1·00
N3	14·90	15·46	0·470	0·496	15·46	1·00
N7	28·09	14·85	0·763	0·825	20·3	1·37
N8	20·35	15·3	0·587	0·661	17·2	1·12
N9	12·20	10·42	0·470	0·496	14·75	1·42

TABLE 8

Calculated Stresses at Quilted Failure

Specimen Number	Failing Load (tons) L	$\dfrac{b}{t_1}$	Cross-Sectional Area of Flat Skin (sq. in.) A_s	Cross-Sectional Area of Corrugations (sq. in.) A_c	Calculated Stress in Skin at Failure (ton/sq. in.) f_s	Calculated Stress in Corrugations at Failure (ton/sq. in.) f_c	$\dfrac{f_c}{f_s}$
E1	34·0	28·8	1·0	1·03	16·7	16·7	1·0
E3	23·8	37·5	0·768	0·826	13·8	15·9	1·15
E5	16·05	46·9	0·614	0·619	11·2	14·7	1·31
E7	33·2	28·8	1·0	1·03	16·3	16·3	1·0
E9	22·25	37·5	0·768	0·826	13·2	14·6	1·1
E11	17·3	46·9	0·614	0·619	11·85	16·05	1·35
E13	40·7	28·8	1·0	1·03	19·5	20·5	1·05
E15	28·9	37·5	0·768	0·826	16·2	20·1	1·24
E17	18·5	46·9	0·614	0·619	12·4	17·5	1·41
E19	42·2	28·8	1·0	1·03	20·0	21·4	1·07
E21	28·4	37·5	0·768	0·826	16·0	19·8	1·24
E23	19·05	46·9	0·614	0·619	12·75	18·25	1·43
E26	24·84	37·5	0·768	0·826	14·4	16·7	1·16
N1	30·24	21·7	0·763	0·825	18·9	18·9	1·0
N4	29·88	21·7	0·763	0·825	18·8	18·8	1·0
N5	24·64	28·2	0·587	0·661	19·7	19·8	1·0
N6	15·94	35·2	0·470	0·496	15·5	17·5	1·13
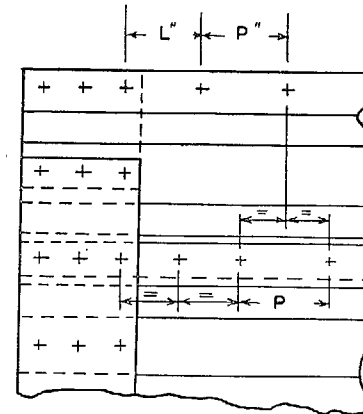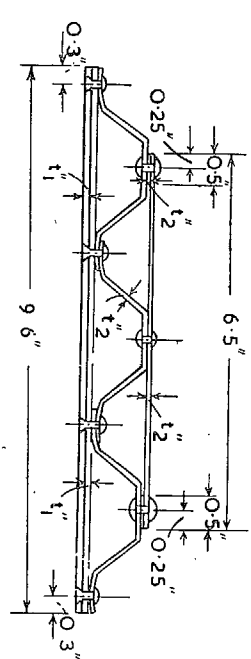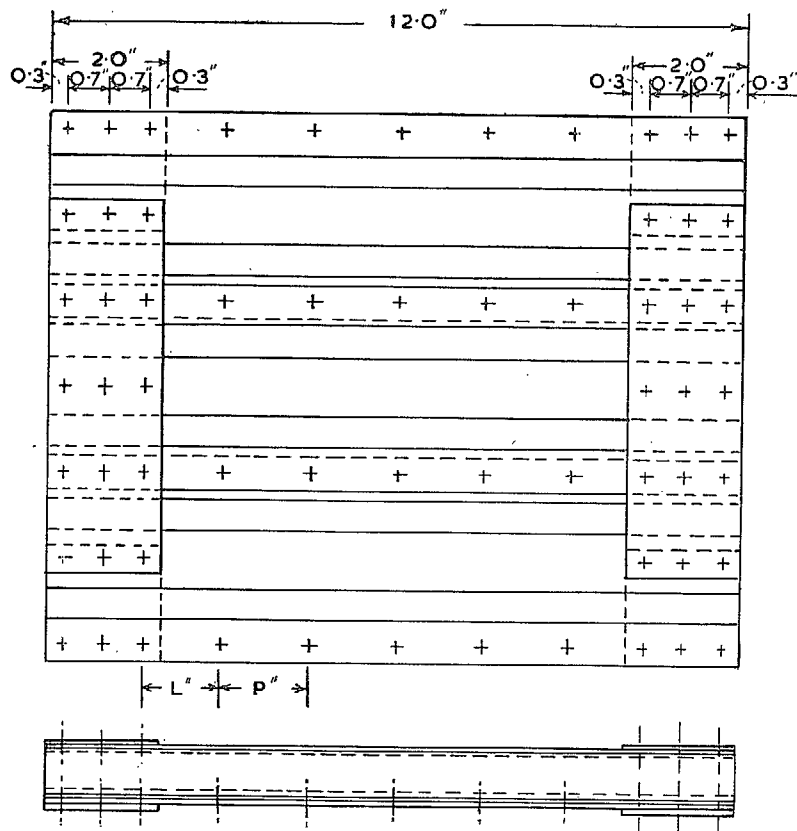
SCRAP VIEW SHOWING ARRANGEMENT
OF STAGGERED RIVETS

ALL RIVETS = $\frac{1}{8}''$ DIAMETER
P = RIVET PITCH
L = 0·55″ FOR P=0·75″
L = 1·3 FOR P=1·5″
VALUES OF P, t_1, AND t_2 ARE GIVEN IN TABLE I
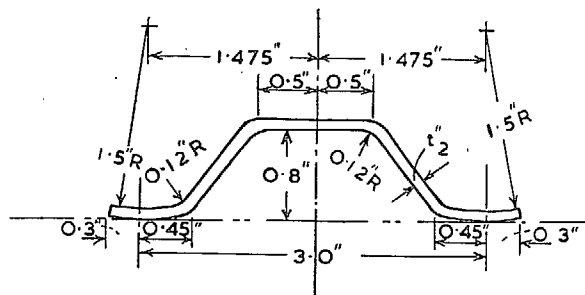
Fig. 1.   General arrangement of typical panel.

DETAIL OF CORRUGATION

FIG. 2. General arrangement of typical panel.

DETAIL OF CORRUGATION

FOR RIVET DIMENSIONS SEE TABLE I

☐ – UNSTAGGERED RIVETS, 0.75"PITCH –E1.
△ – UNSTAGGERED RIVETS, 1.5° PITCH –E2.
○ – STAGGERED RIVETS, 0.75"PITCH –E7.
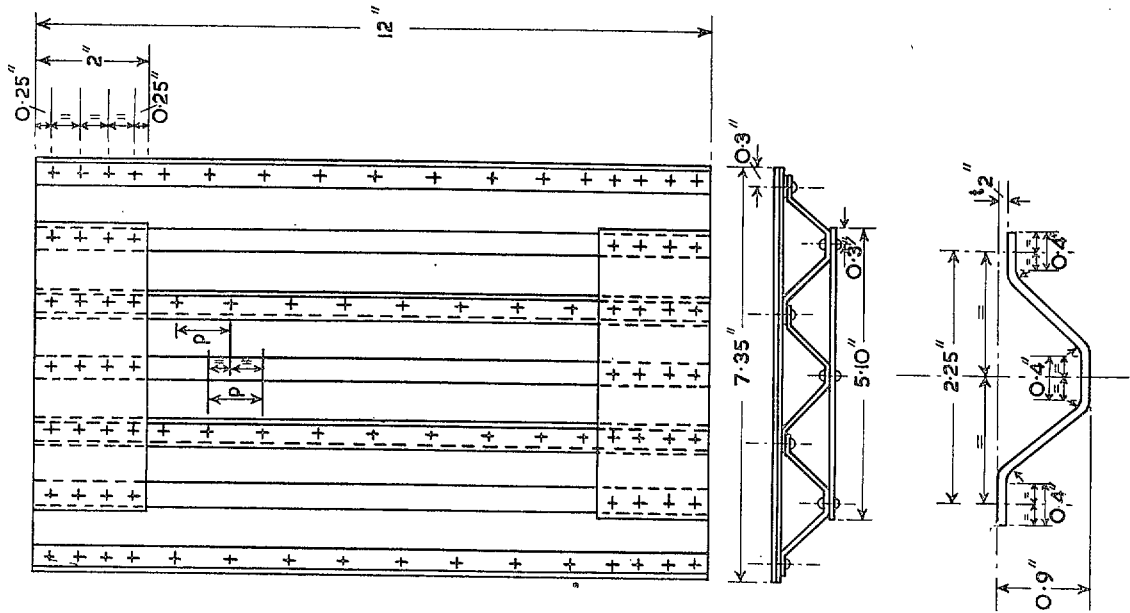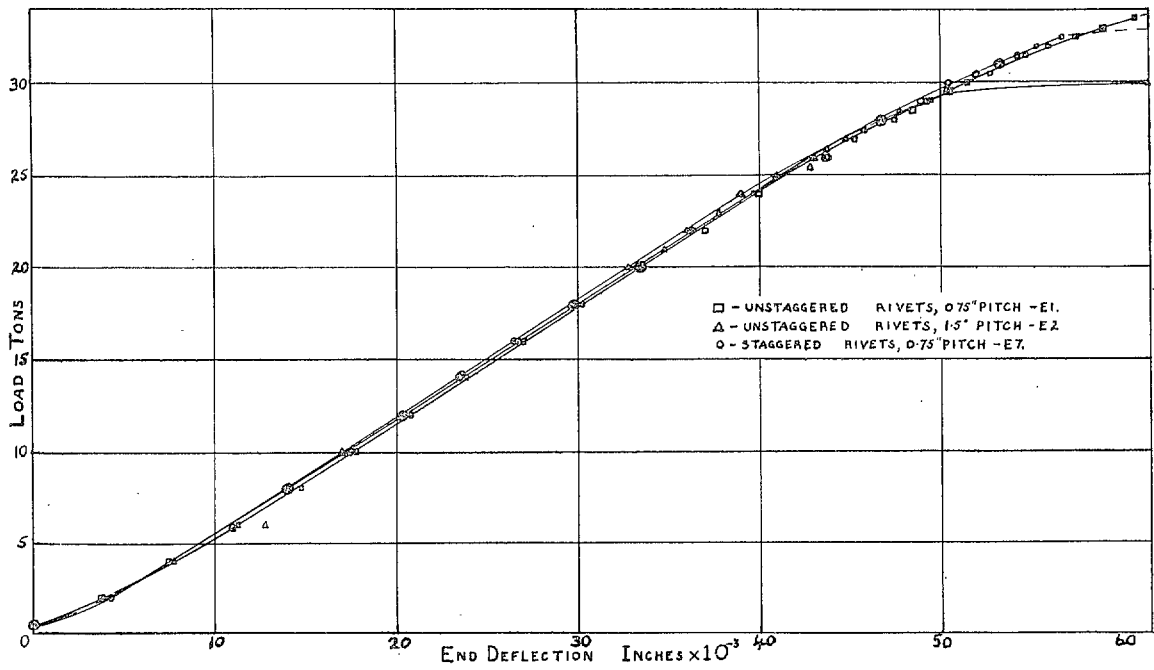
FIG. 3. Load-deflection curves—12 s.w.g./14 s.w.g. combinations.
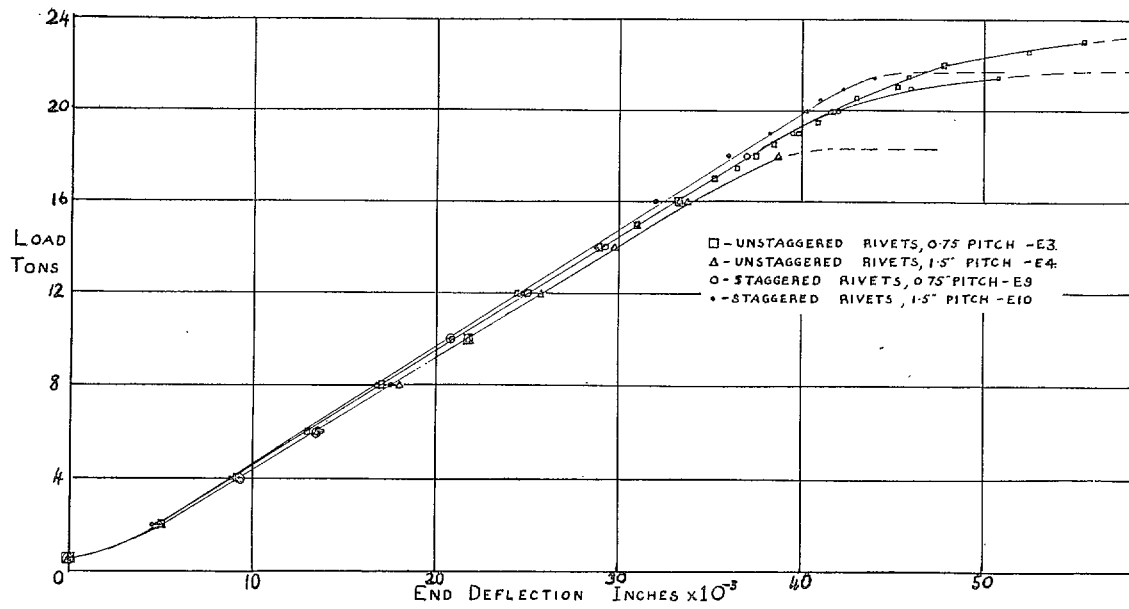
FIG. 4. Load-deflection curves—14 s.w.g./16 s.w.g. combinations.
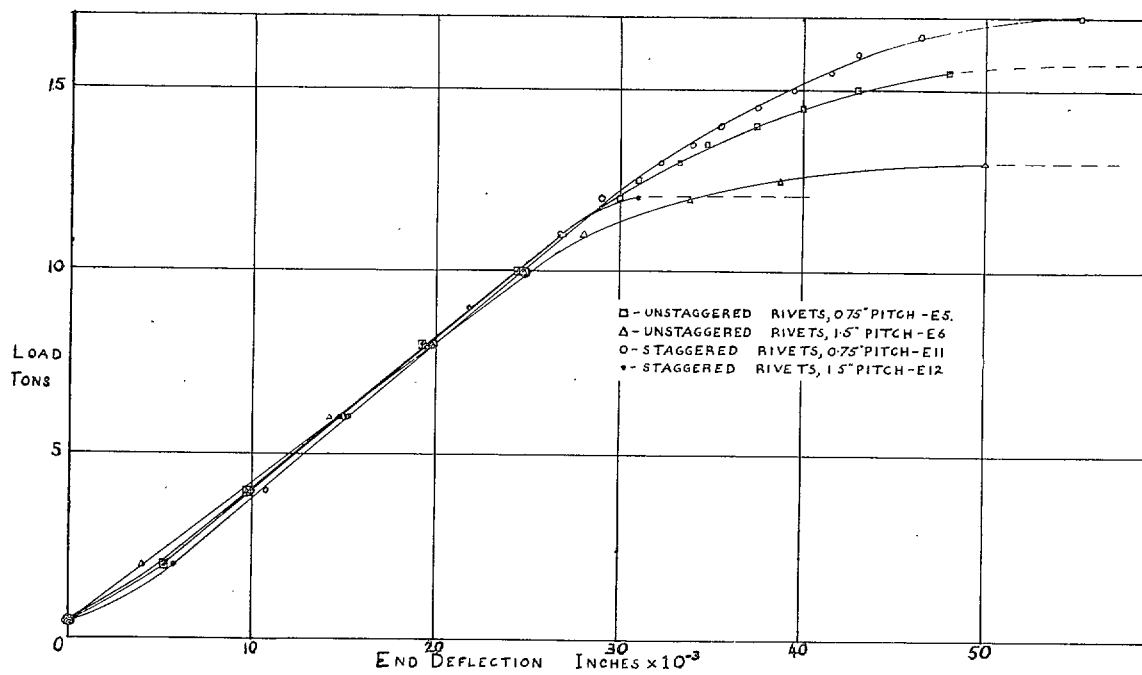
FIG. 5. Load-deflection curves—16 s.w.g./18 s.w.g. combinations.

19
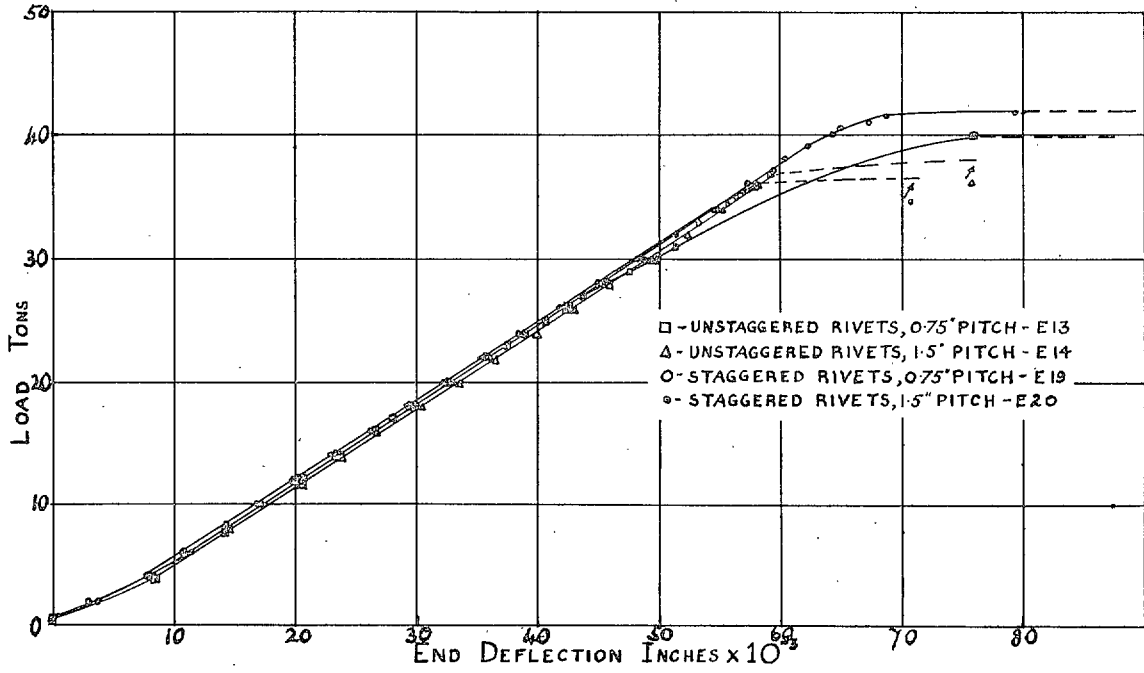
FIG. 6.   Load-deflection curves—12 s.w.g./14 s.w.g. combinations.
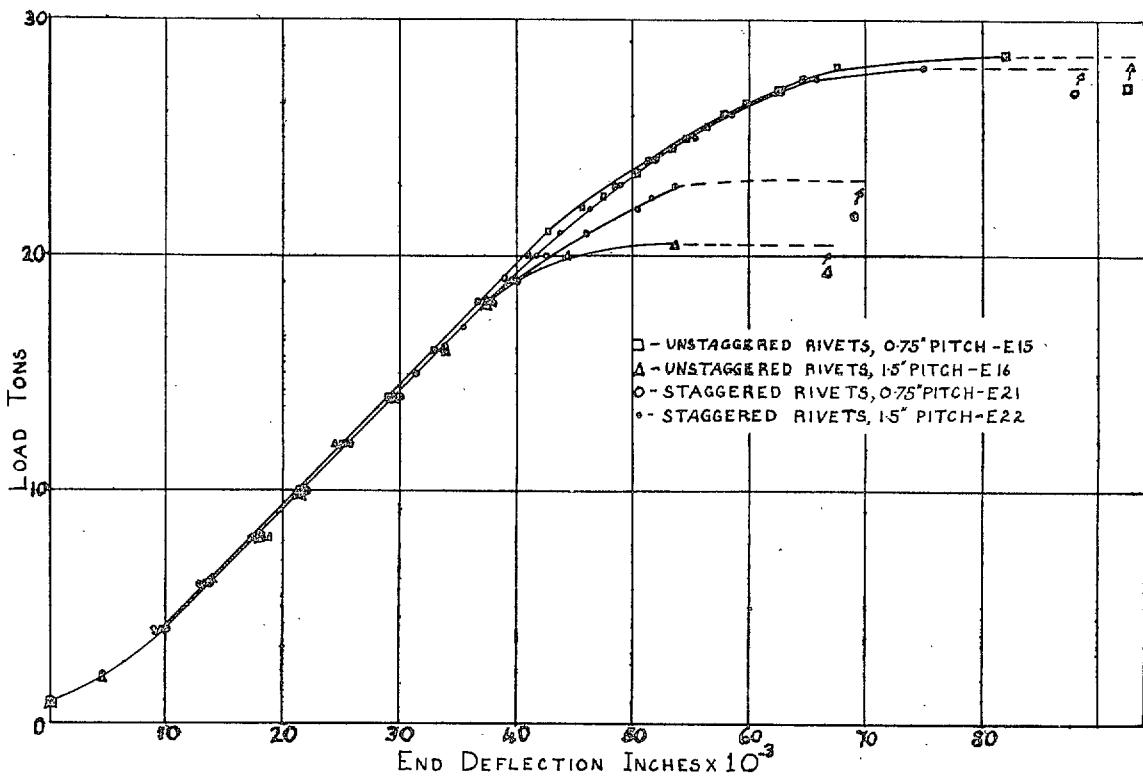
FIG. 7.   Load-deflection curves—14 s.w.g./16 s.w.g. combinations.

20
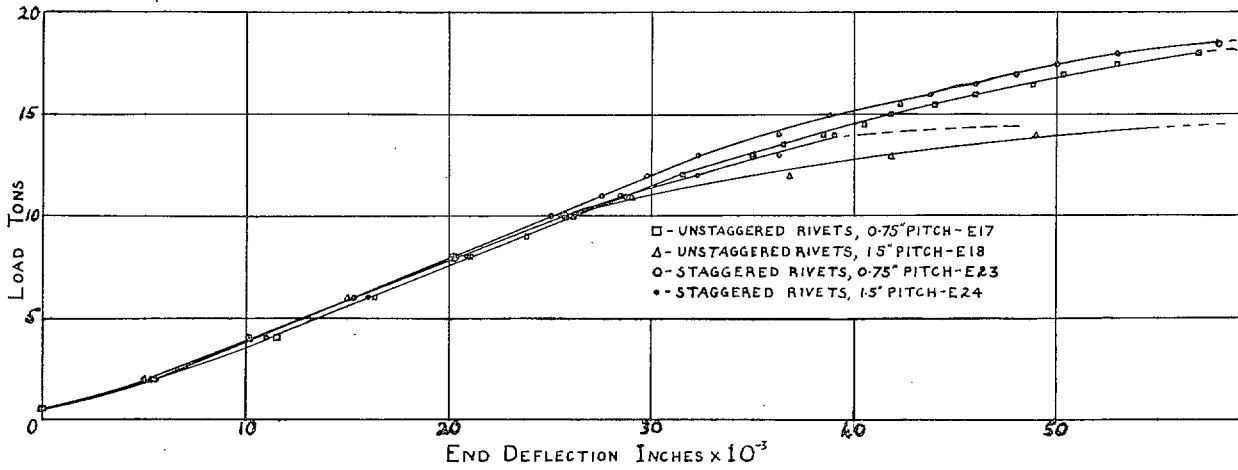
FIG. 8. Load-deflection curves—16 S.W.G./18 S.W.G. combinations.
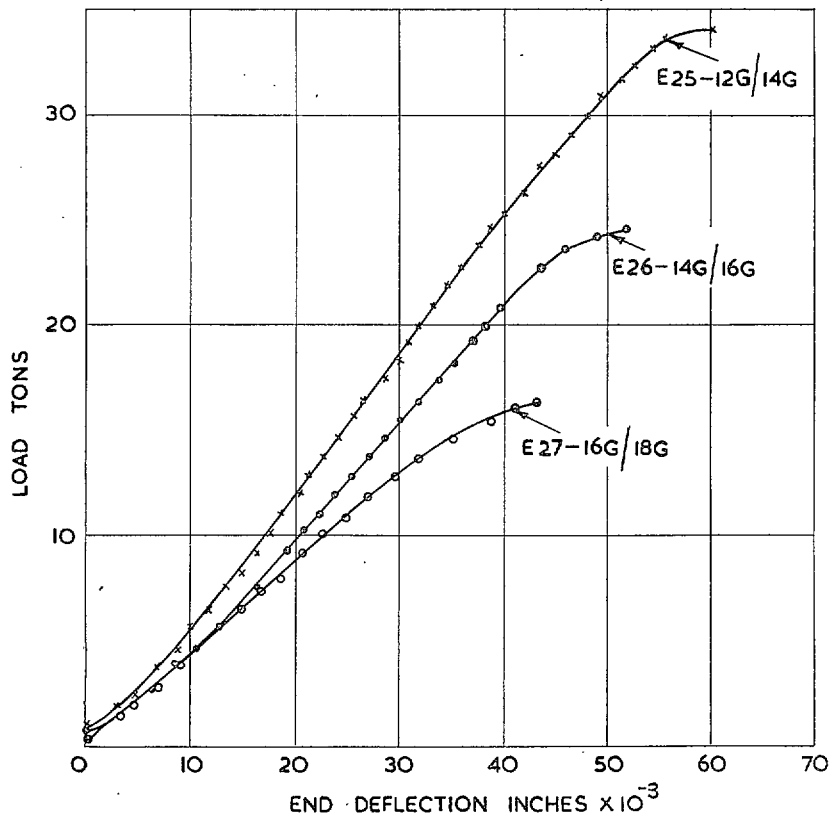
FIG. 9. Load-deflection curves E25/E27.

21
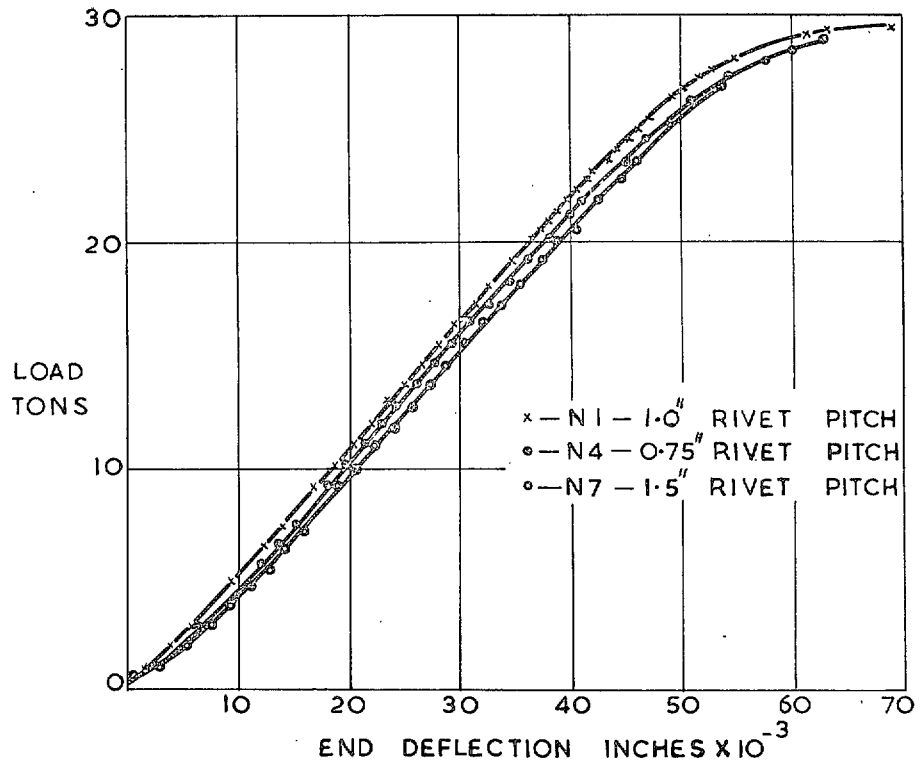
FIG. 10.   Load-deflection curves—12 S.W.G./14 S.W.G. combinations.
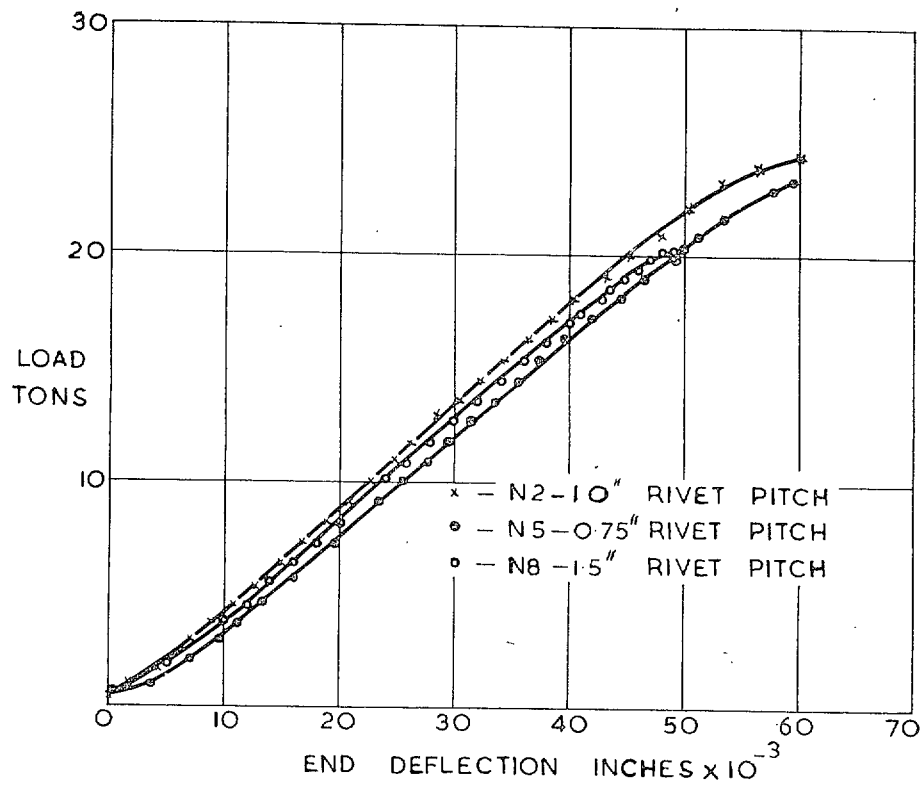
FIG. 11.   Load-deflection curves—14 S.W.G./16 S.W.G. combinations.
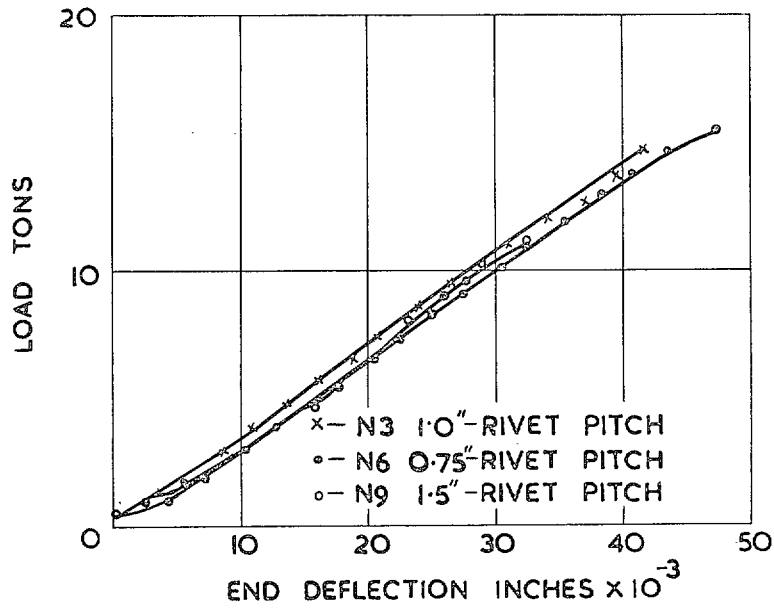
FIG. 12.   Load-deflection curves—16 S.W.G./18 S.W.G. combinations.
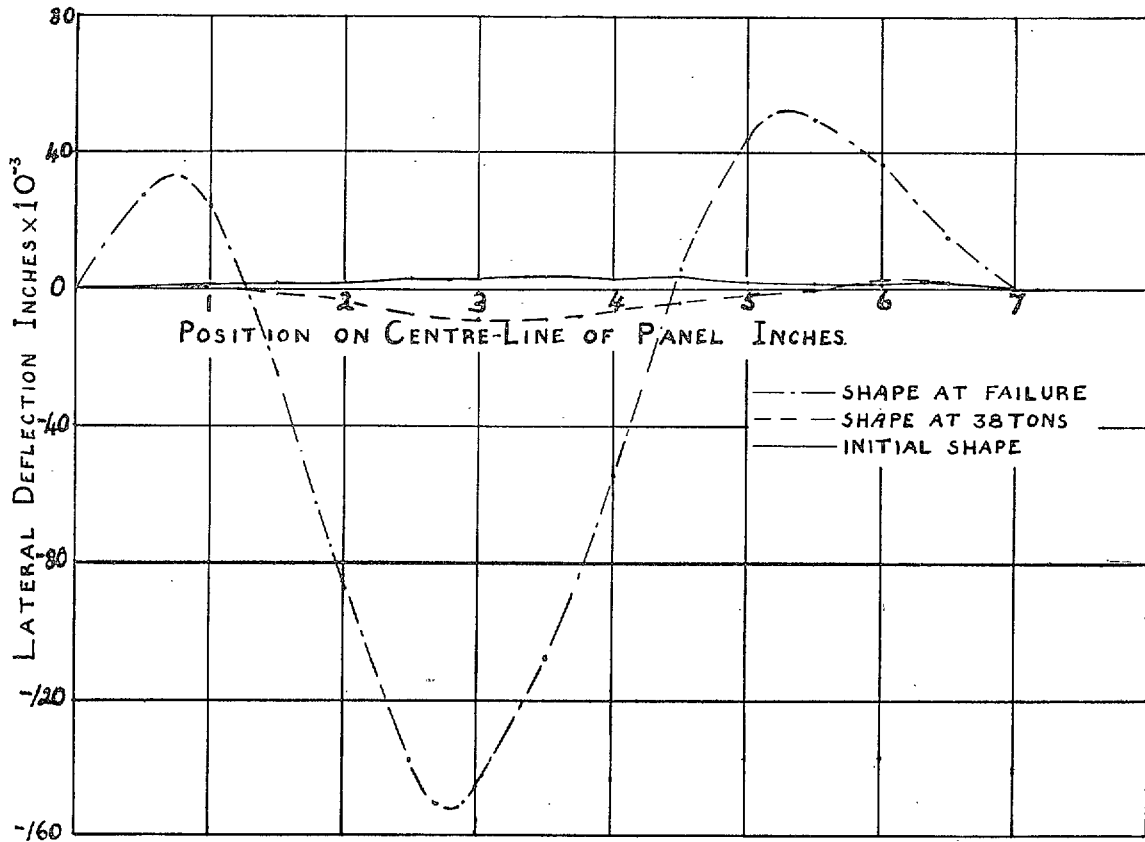
FIG. 13.   Specimen Number E19—profiles.
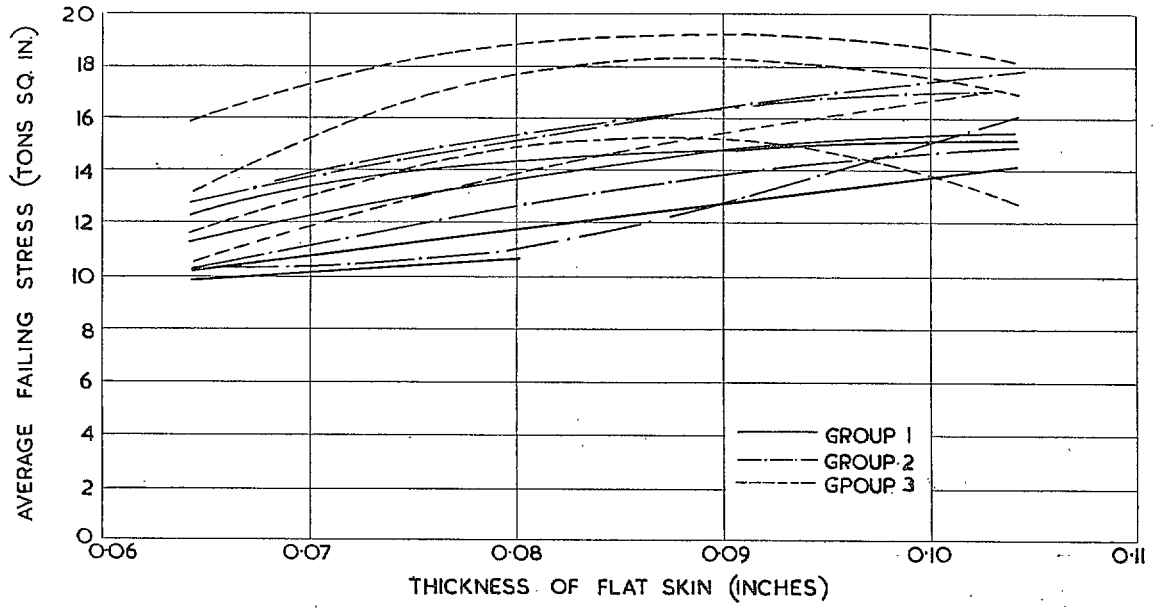
FIG. 14.   Average failing stresses.
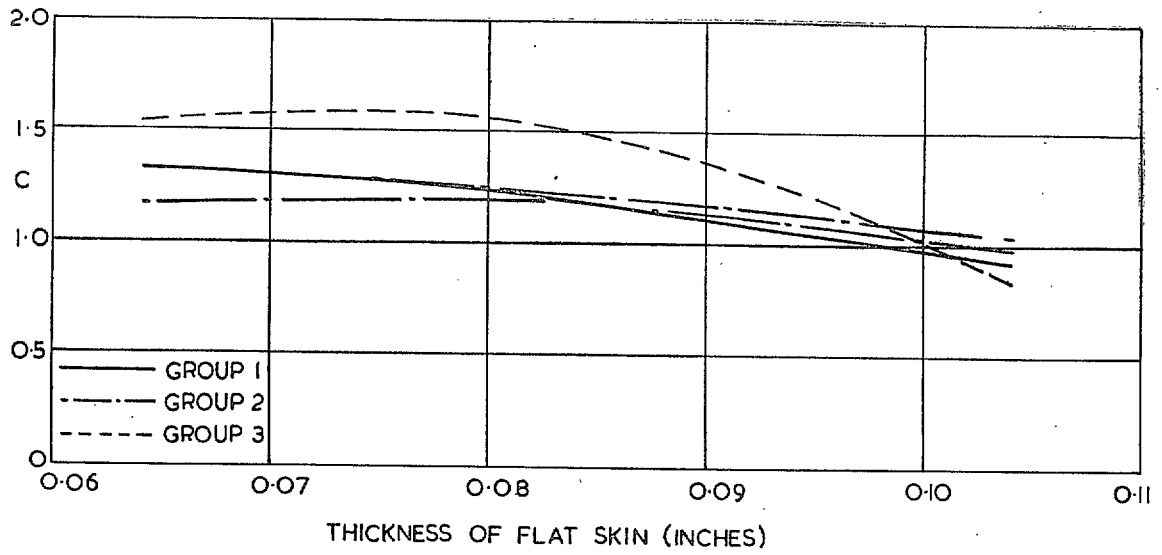
FIG. 15.   Inter-rivet buckling—*C*.

24
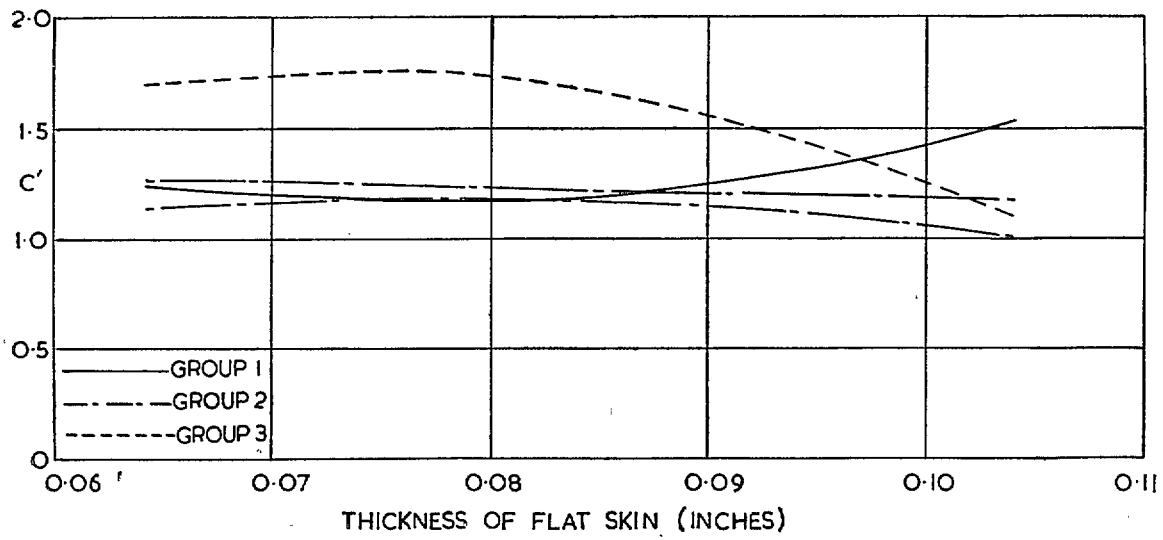
FIG. 16.   Inter-rivet buckling—C'.
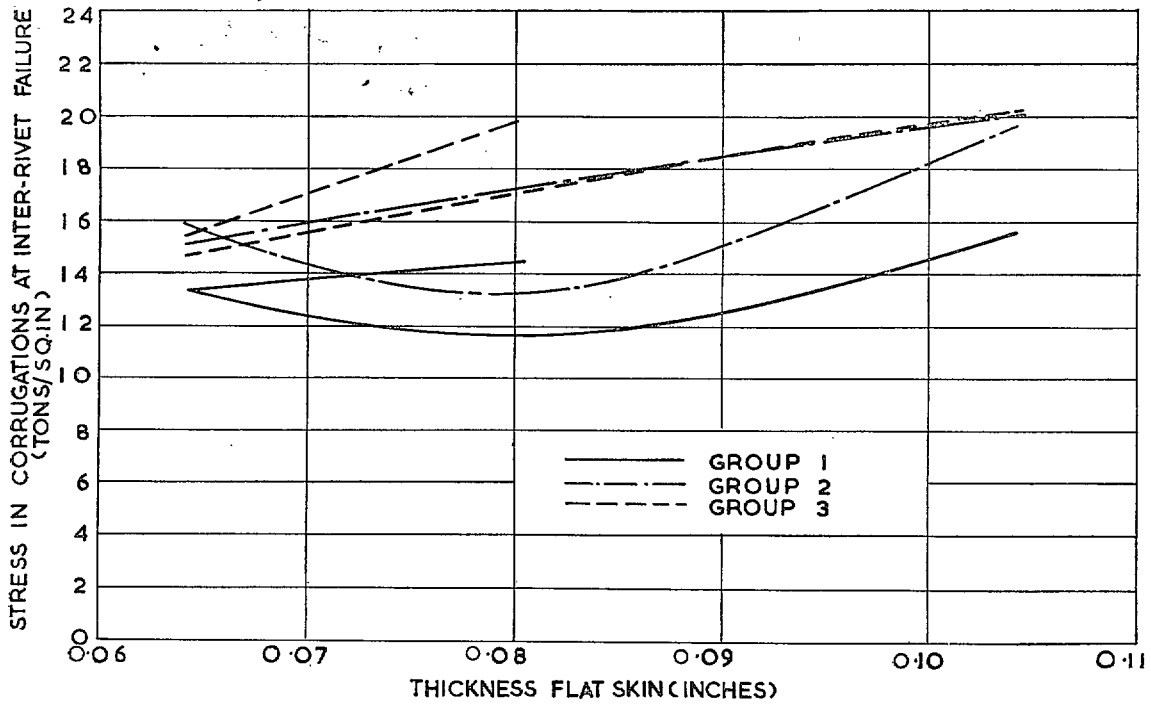
FIG. 17.   Inter-rivet failure.

25

C
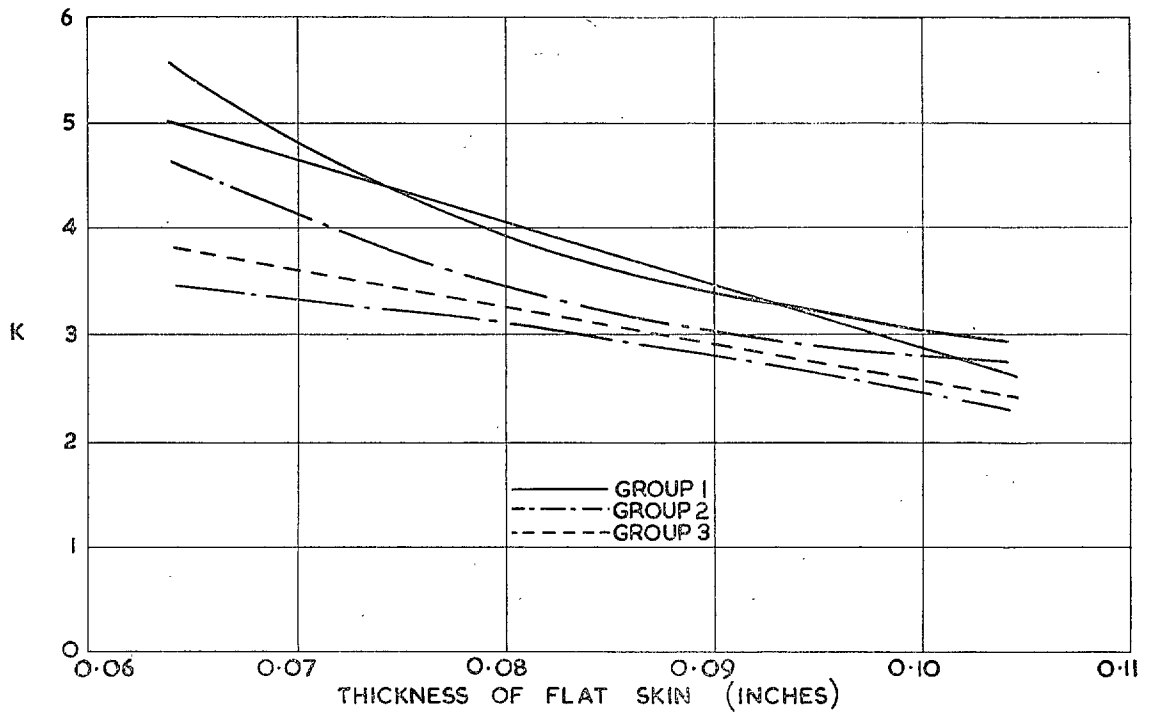
FIG. 18.   Quilted buckling—K.
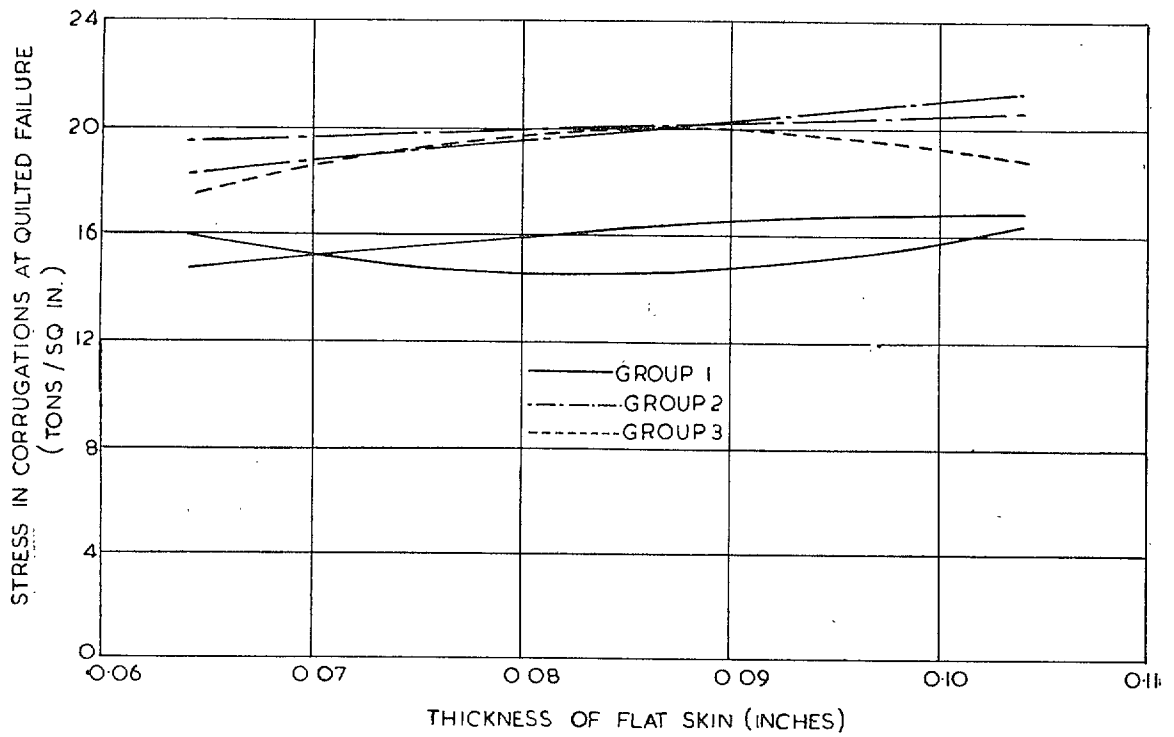
FIG. 19.   Quilted failure.

26
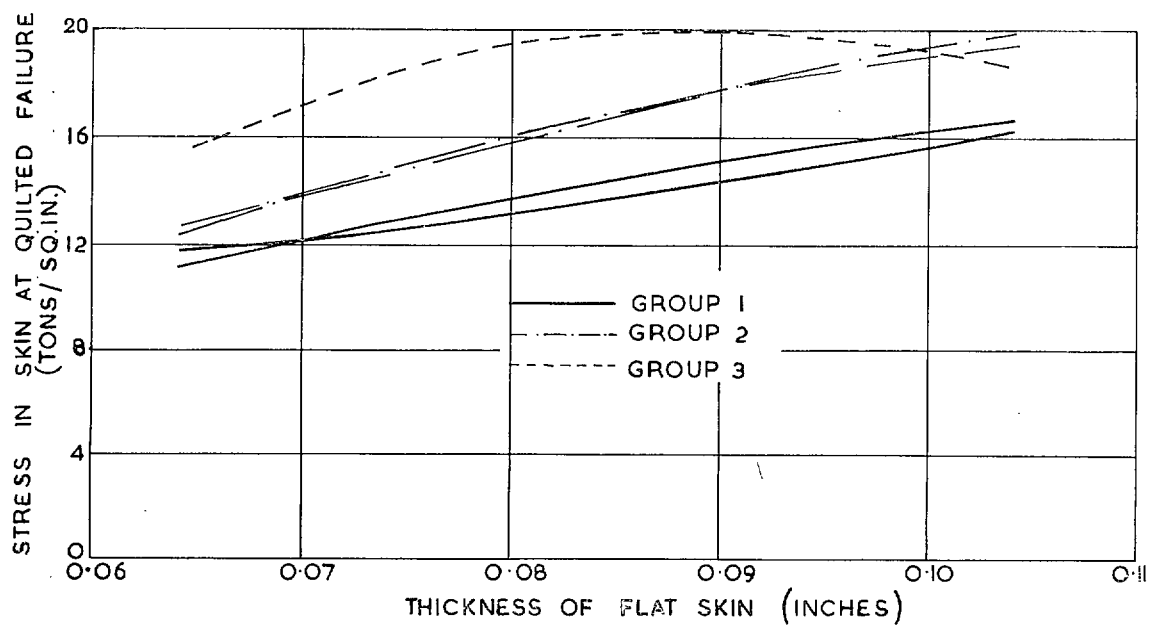
FIG. 20.   Quilted failure.
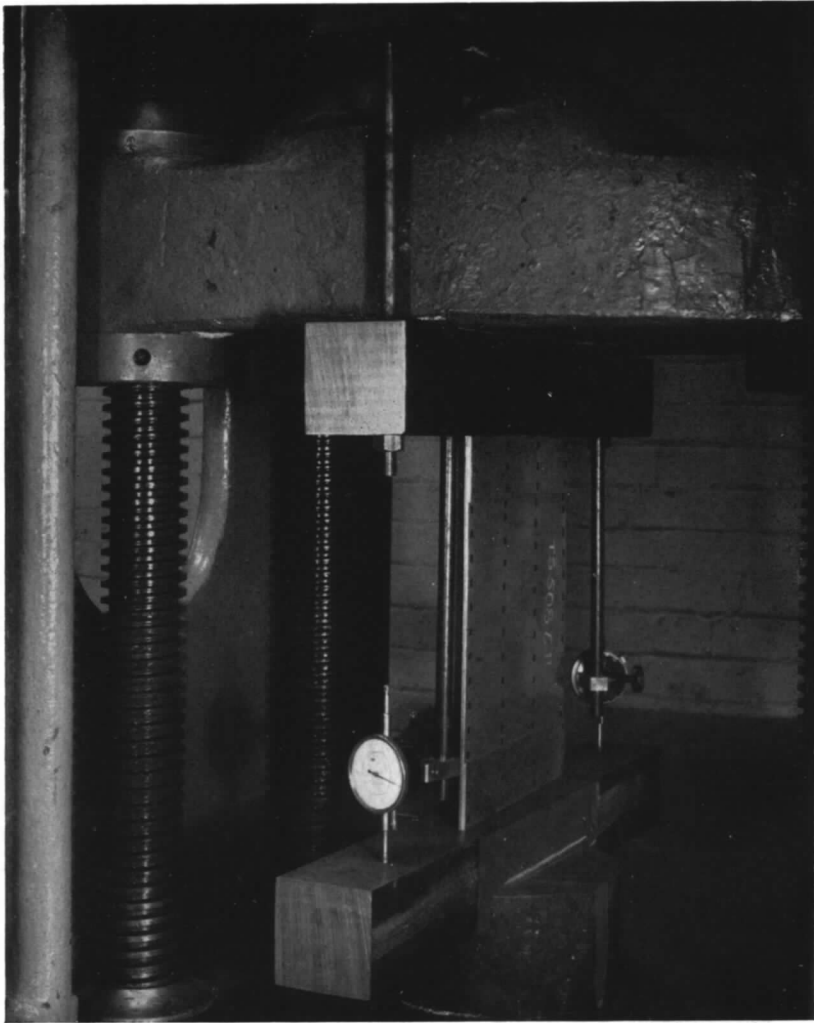
FIG. 21. Test rig showing method of measuring end deflections.
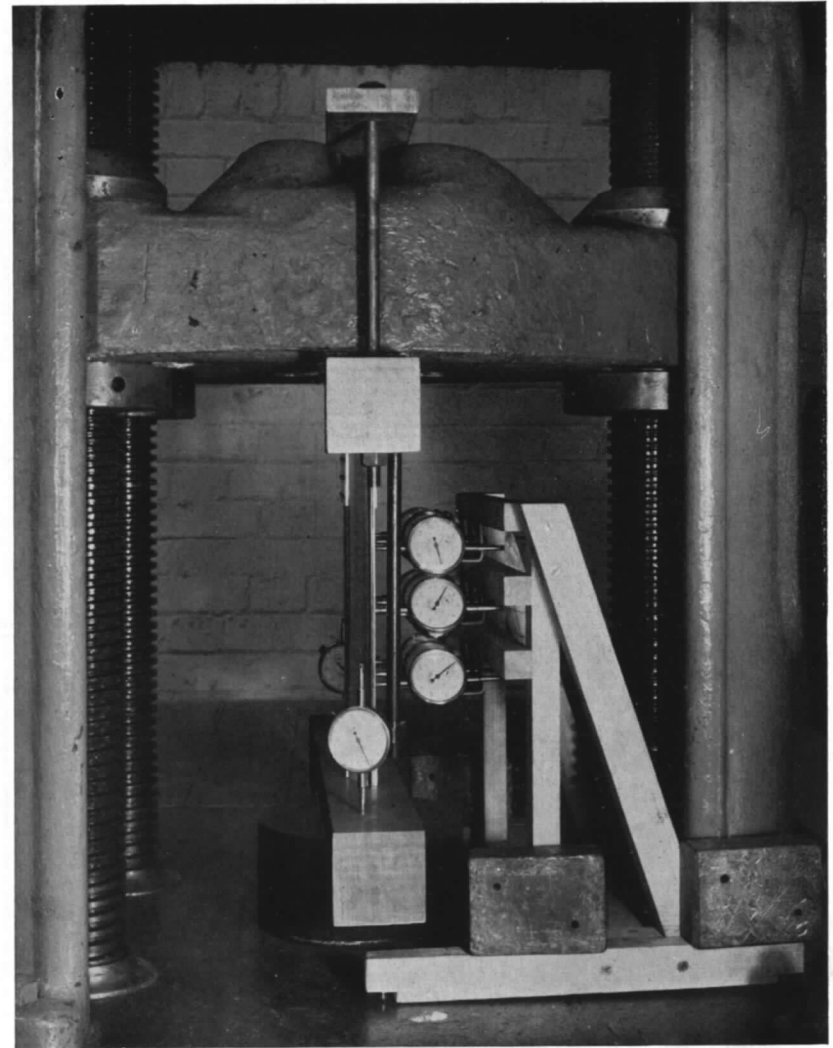
FIG. 22. Test rig showing method of measuring lateral deflections.
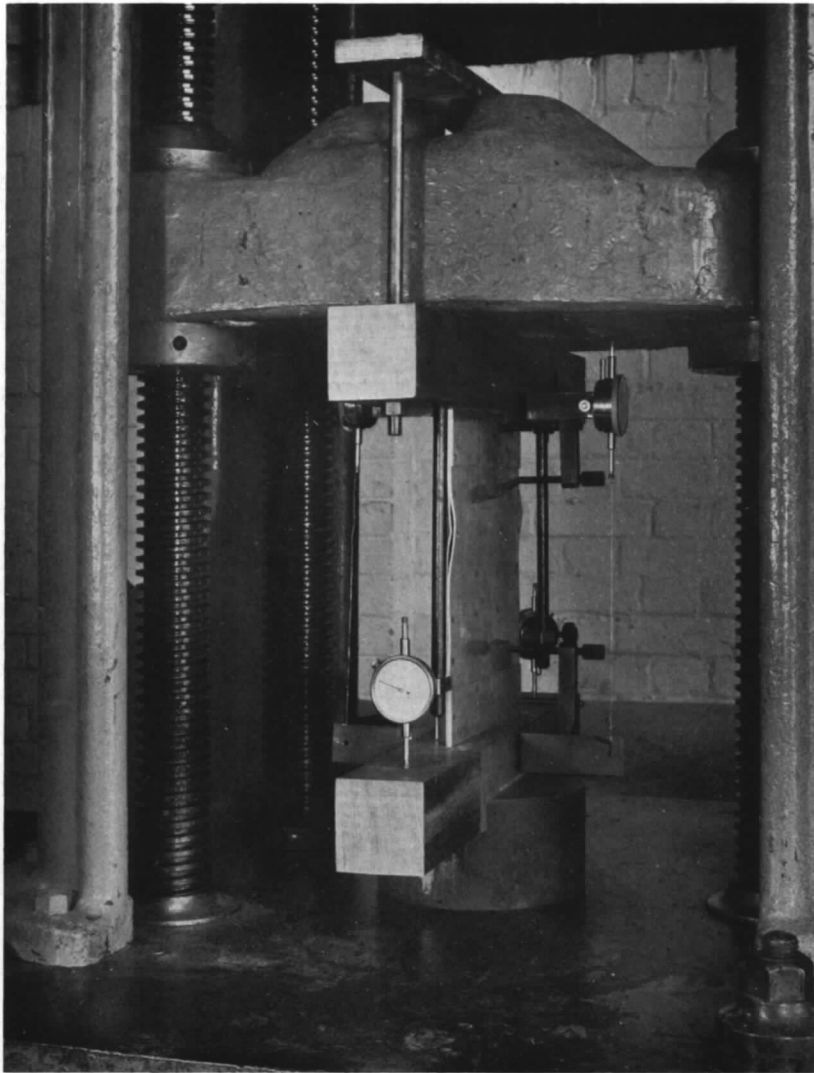
FIG. 23. Test rig showing positions of dials on specimen Number E18.
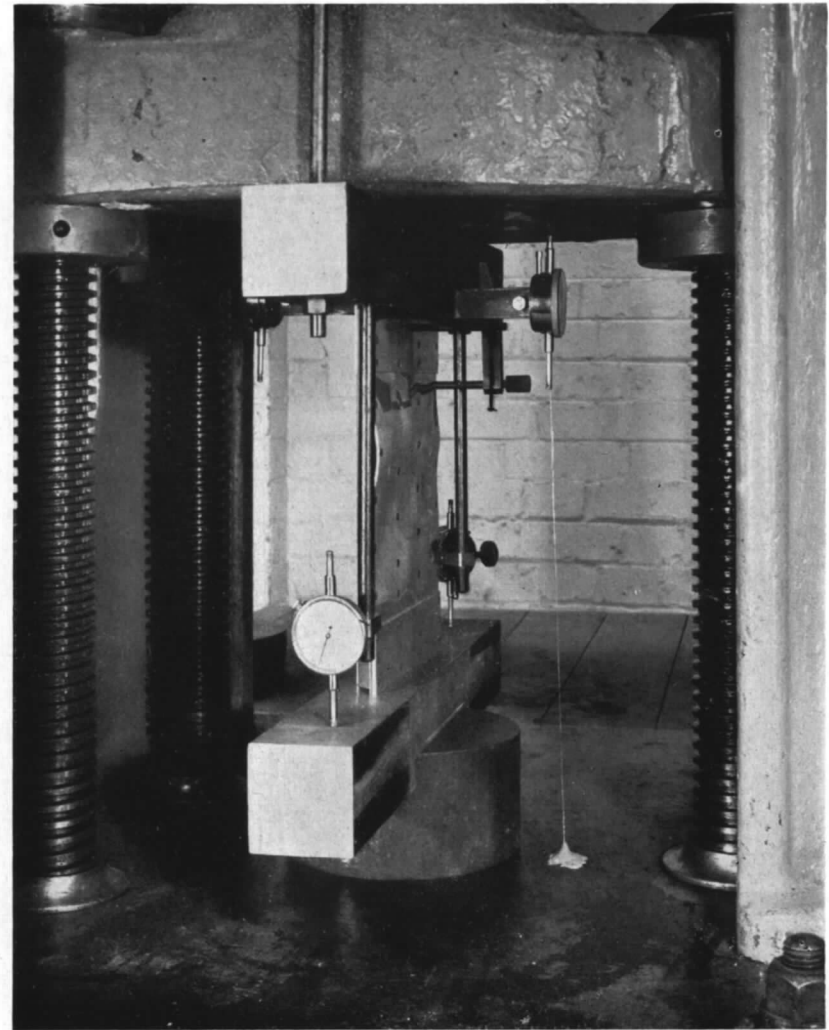
FIG. 24. Test rig showing positions of dials on specimen Number E24.
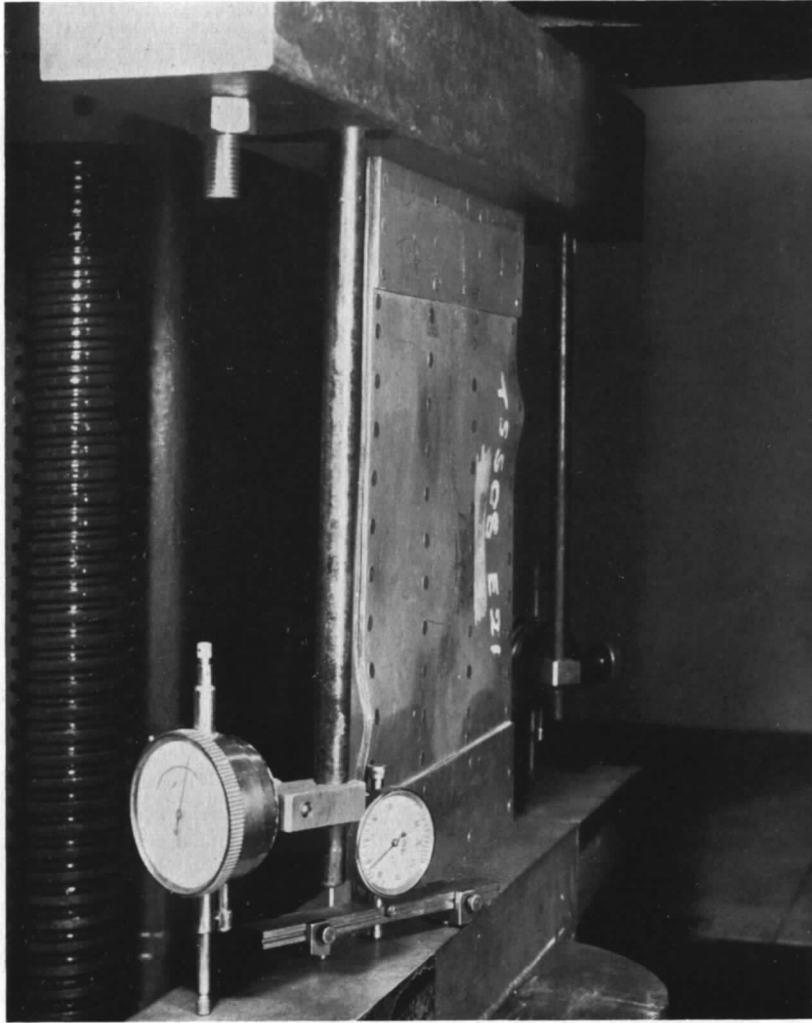
FIG. 25. Specimen Number E21 showing typical quilted failure and travelling gauge.
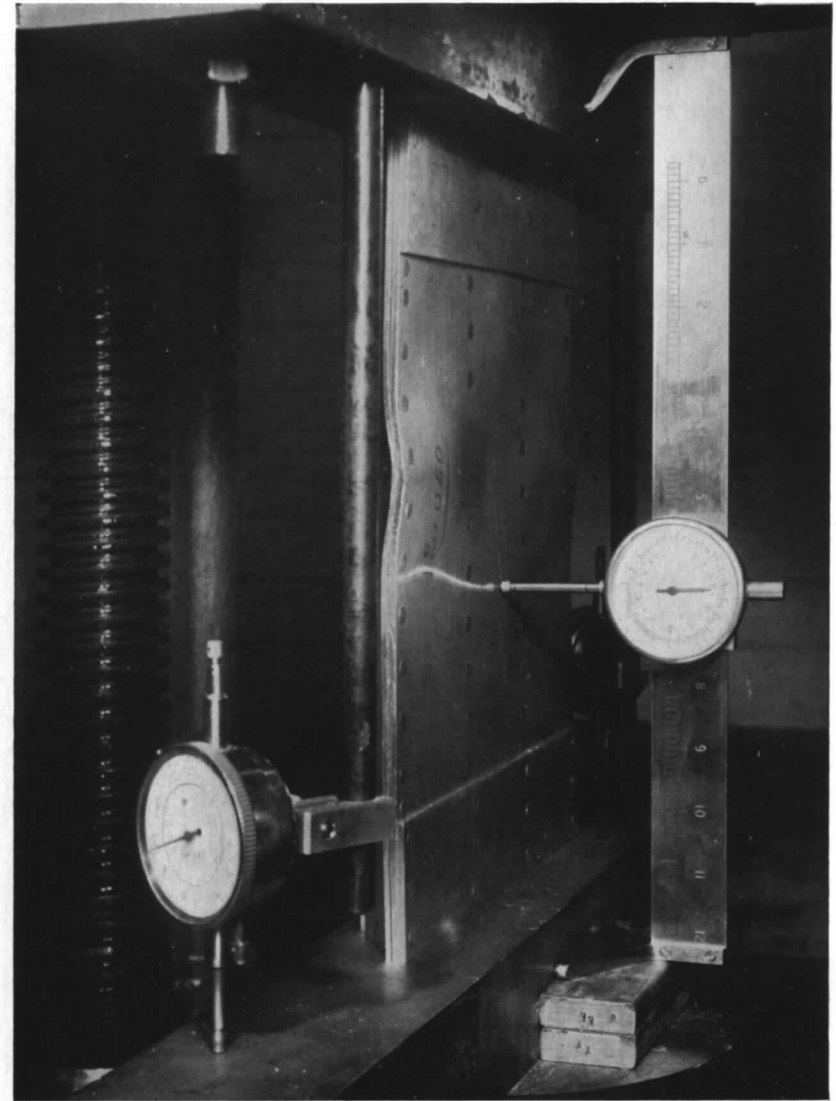
FIG. 26. Test rig showing traverse gauge.

FIG. 27. Specimen Number E2 showing typical inter-rivet failure for unstaggered rivets.

FIG. 28. Specimen Number E10 showing typical diagonal inter-rivet failure for staggered rivets.
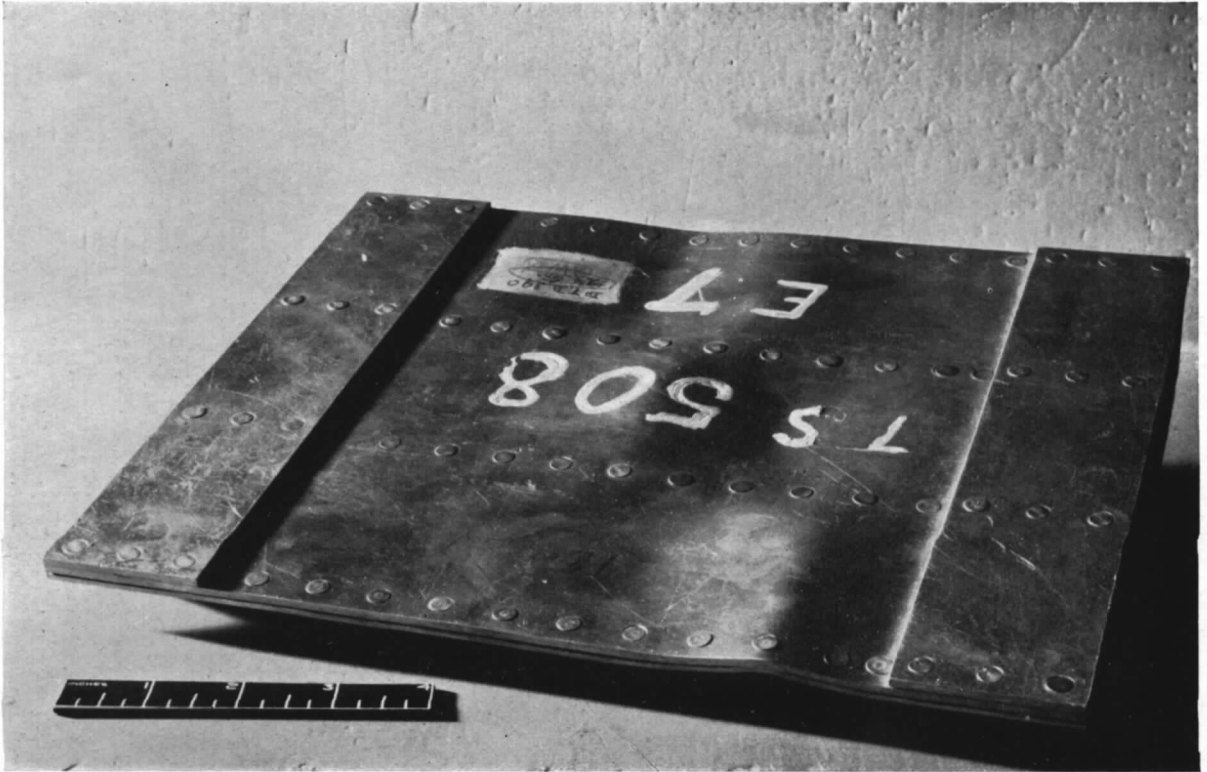
FIG. 29. Specimen Number E7 showing typical quilted failure (staggered rivets).
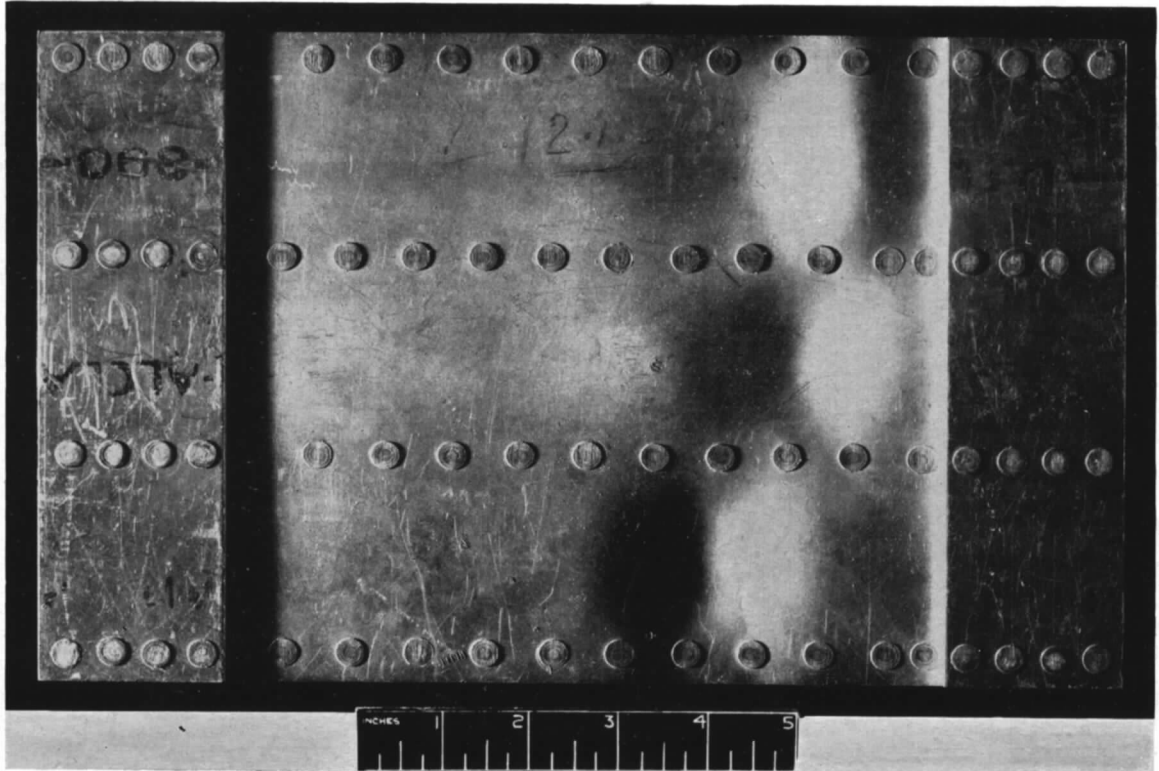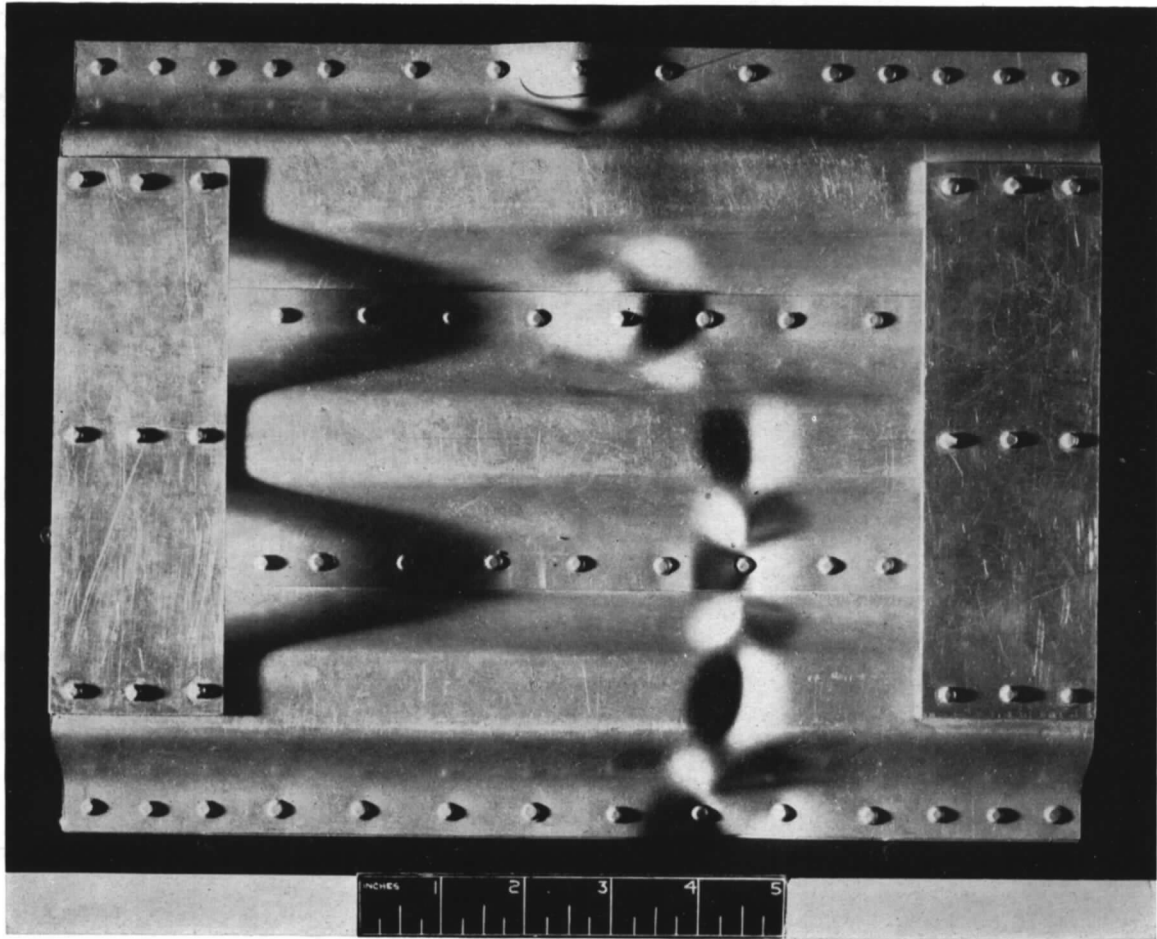

FIG. 30. Panel failure.

FIG. 31.   Panel failure.

33

Publications of the

Aeronautical Research Council

ANNUAL TECHNICAL REPORTS OF THE AERONAUTICAL RESEARCH COUNCIL (BOUND VOLUMES)—

1934-35 Vol. I. Aerodynamics. *Out of print.*
Vol. II. Seaplanes, Structures, Engines, Materials, etc. 40s. (40s. 8d.)

1935-36 Vol. I. Aerodynamics. 30s. (30s. 7d.)
Vol. II. Structures, Flutter, Engines, Seaplanes, etc. 30s. (30s. 7d.)

1936 Vol. I. Aerodynamics General, Performance, Airscrews, Flutter and Spinning. 40s. (40s. 9d.)
Vol. II. Stability and Control, Structures, Seaplanes, Engines, etc. 50s. (50s. 10d.)

1937 Vol. I. Aerodynamics General, Performance, Airscrews, Flutter and Spinning. 40s. (40s. 10d.)
Vol. II. Stability and Control, Structures, Seaplanes, Engines, etc. 60s. (61s.)

1938 Vol. I. Aerodynamics General, Performance, Airscrews. 50s. (51s.)
Vol. II. Stability and Control, Flutter, Structures, Seaplanes, Wind Tunnels, Materials. 30s. (30s. 9d.)

1939 Vol. I. Aerodynamics General, Performance, Airscrews, Engines. 50s. (50s. 11d.)
Vol. II. Stability and Control, Flutter and Vibration, Instruments, Structures, Seaplanes, etc. 63s. (64s. 2d.)

1940 Aero and Hydrodynamics, Aerofoils, Airscrews, Engines, Flutter, Icing, Stability and Control, Structures, and a miscellaneous section. 50s. (51s.)

Certain other reports proper to the 1940 volume will subsequently be included in a separate volume.

ANNUAL REPORTS OF THE AERONAUTICAL RESEARCH COUNCIL—

1933-34	1s. 6d. (1s. 8d.)
1934-35	1s. 6d. (1s. 8d.)
April 1, 1935 to December 31, 1936.	4s. (4s. 4d.)
1937	2s. (2s. 2d.)
1938	1s. 6d. (1s. 8d.)
1939-48	3s. (3s. 2d.)

INDEX TO ALL REPORTS AND MEMORANDA PUBLISHED IN THE ANNUAL TECHNICAL REPORTS, AND SEPARATELY—

April, 1950   R. & M. No. 2600.   2s. 6d. (2s. 7½d.)

INDEXES TO THE TECHNICAL REPORTS OF THE AERONAUTICAL RESEARCH COUNCIL—

December 1, 1936 — June 30, 1939.	R. & M. No. 1850.	1s. 3d. (1s. 4½d.)
July 1, 1939 — June 30, 1945.	R. & M. No. 1950.	1s. (1s. 1½d.)
July 1, 1945 — June 30, 1946.	R. & M. No. 2050.	1s. (1s. 1½d.)
July 1, 1946 — December 31, 1946.	R. & M. No. 2150.	1s. 3d. (1s. 4½d.)
January 1, 1947 — June 30, 1947.	R. & M. No. 2250.	1s. 3d. (1s. 4½d.)

Prices in brackets include postage.

Obtainable from

HIS MAJESTY'S STATIONERY OFFICE

or through any bookseller.